IEEE CSC & ESAS SUPERCONDUCTIVITY NEWS FORUM (global edition), April 2020.
Plenary presentation PL5-INV given at ISS, 3-5 December 2019, Kyoto, Japan..

UNIVERSITÉ DE GENÈVE
FACULTÉ DES SCIENCES

DQMP
http://supra.unige.ch

32nd International Symposium on Superconductivity
ISS 2019

FNSNF
FONDS NATIONAL SUISSE DE LA RECHERCHE SCIENTIFIQUE

Frontiers of Nb_3Sn wire technology

Carmine SENATORE

Department of Quantum Matter Physics
University of Geneva, Switzerland

With special thanks to René Flükiger (UNIGE) for having introduced me to the field of Nb_3Sn, Amalia Ballarino, Bernardo Bordini, Luca Bottura and Davide Tommasini (CERN) for the exciting collaboration in view of the FCC, Davide Uglietti (EPFL) for his interesting suggestions and my great team at UNIGE, Florin Buta, Christian Barth, Jose Ferradas, Tommaso Bagni, Marco Bonura, Gianmarco Bovone, Davide Matera and Damien Zurmuehle

Outline

A brief introduction to A15 superconductors

Nb_3Sn: the pathway to industrialization

Towards the ultimate performance of Nb_3Sn

- ***the Future Circular Collider study @ CERN***

Not only critical current !!

- ***Focus on the electromechanical properties***

Outline

A brief introduction to A15 superconductors

Nb_3Sn: the pathway to industrialization

Towards the ultimate performance of Nb_3Sn

- ***the Future Circular Collider study @ CERN***

Not only critical current !!

- ***Focus on the electromechanical properties***

An introduction to A15 superconductors

- ***A15 are intermetallic compounds with A_3B formula***
- ***V_3Si is the earliest example, T_c = 17.1 K (Hardy, 1954)***

PHYSICAL REVIEW VOLUME 93, NUMBER 5 MARCH 1, 1954

The Superconductivity of Some Transition Metal Compounds*

GEORGE F. HARDY† AND JOHN K. HULM
Institute for the Study of Metals, University of Chicago, Chicago, Illinois
(Received November 23, 1953)

About eighty transition metal compounds comprising borides, carbides, nitrides, oxides, silicides, and germanides of metals of Groups 4A, 5A, and 6A were tested for superconductivity down to 1.20°K, using a magnetic method. Among the specimens were most of the known compounds of the above type not examined ... superconducting behavior by previous workers, and in all cases the structures ... The following eleven new superconductors were discovered, ... parentheses: W_2B (3.10°), Nb_2C (9.18°), Ta_2C (3.26°), ... (1.30°), Mo_3Ge (1.43°), α-$ThSi_2$ (3.16°), β-$ThSi_2$ (2.41°), ... include the first superconducting germanides, V_3Ge and Mo_3Ge, which, together with V_3Si and Mo_3Si, crystallize in the cubic β-tungsten structure. The transition temperature of V_3Si is apparently the highest known for any binary superconducting compound.

V_3Si (17.1°)

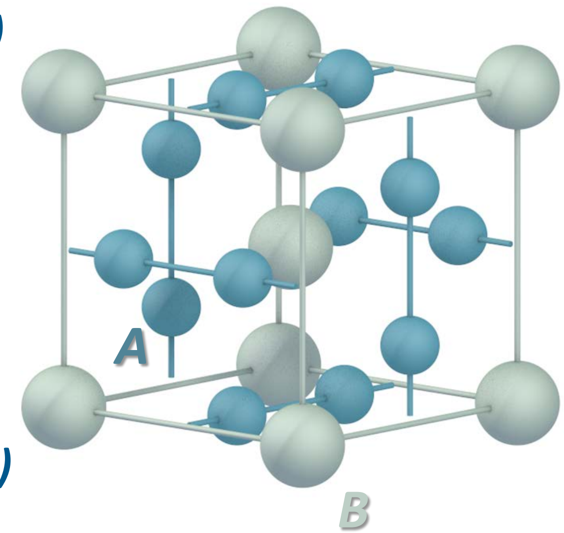

- ***Nb_3Sn came 6 month later, T_c = 18 K (Matthias, 1954)***

PHYSICAL REVIEW VOLUME 95, NUMBER 6 SEPTEMBER 15, 1954

Superconductivity of Nb_3Sn

B. T. MATTHIAS, T. H. GEBALLE, S. GELLER, AND E. CORENZWIT
Bell Telephone Laboratories, Murray Hill, New Jersey
(Received June 10, 1954)

Intermetallic compounds of niobium and tantalum with tin have been found. The superconducting transition ... one known.

Nb_3Sn at 18°K

VOLUME 6, NUMBER 3 PHYSICAL REVIEW LETTERS FEBRUARY 1, 1961

SUPERCONDUCTIVITY IN Nb_3Sn AT HIGH CURRENT DENSITY IN A MAGNETIC FIELD OF 88 kgauss

J. E. Kunzler, E. Buehler, F. S. L. Hsu, and J. H. Wernick
Bell Telephone Laboratories, Murray Hill, New Jersey
(Received January 9, 1961)

- ***... and Nb_3Sn exhibited very high in-field J_c (Kunzler, 1961)***

exceeding 100 000 amperes/cm² in magnetic fields as large as 88 kgauss.

An introduction to A15 superconductors

- ***More than 50 superconductors, 10 of them with $T_c \geq 15$ K***

	Ti	Zr	V	Nb	Ta	Cr	Mo
Al			11.8 K	18.8 K			0.6 K
Ga			16.8 K	20.3 K			0.8 K
In			13.9 K	9.2 K			
Tl				9.0 K			
Si			17.1 K	19.0 K			1.7 K
Ge			11.2 K	23.2 K	8.0 K	1.2 K	1.8 K
Sn	5.8 K	0.9 K	7.0 K	18.0 K	8.4 K		
Pb		0.8 K		8.0 K	17.0 K		
As			0.2 K				
Sb	5.8 K		0.8 K	2.2 K			
Bi		3.4 K		4.5 K			
Tc							15.0 K
Re							15.0 K
Ru						3.4 K	10.6 K
Os			5.7 K	1.1 K		4.7 K	12.7 K
Rh			1.0 K	2.6 K	10.0 K	0.3 K	
Ir	5.4 K		1.7 K	3.2 K	6.6 K	0.8 K	9.6 K
Pd			0.08 K				
Pt	0.5 K		3.7 K	10.9 K	0.4 K		8.8 K
Au		0.9 K	3.2 K	11.5 K	16.0 K		

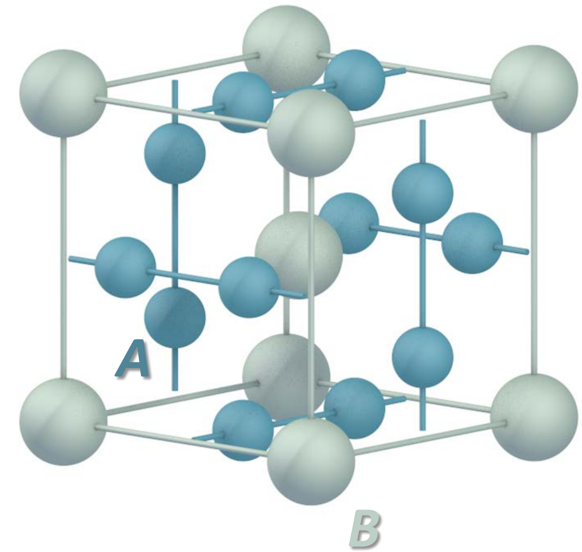

- ***V_3Ga, Nb_3Sn and Nb_3Al can be produced as practical conductors***

- ***Nb_3Ge held the record for the highest T_c (23.2 K) until 1986***

The Nb-Sn phase diagram

Implications for practical conductors

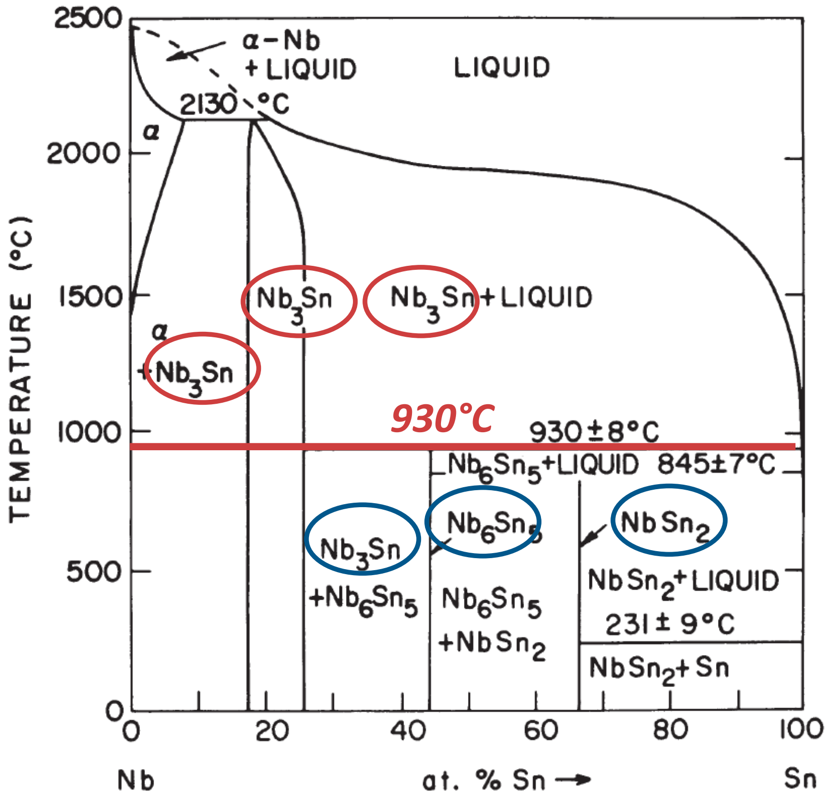

D. P. Charlesworth et al., J. of Mat. Sci. 5 (1970) 580

- Three stable phases: Nb_3Sn, Nb_6Sn_5 and $NbSn_2$
- Below 930°C $NbSn_2$ and Nb_6Sn_5 have a more rapid kinetics of formation
- Above 930°C the only stable phase is Nb_3Sn

The practical consequence of this phase diagram is that the reaction to form Nb_3Sn needs to be performed at T > 930°C

Outline

A brief introduction to A15 superconductors

Nb_3Sn: the pathway to industrialization

Towards the ultimate performance of Nb_3Sn

- *the Future Circular Collider study @ CERN*

Not only critical current !!

- *Focus on the electromechanical properties*

1963-1964: Nb_3Sn coated conductors (!!)

The earliest conductors based on Nb_3Sn

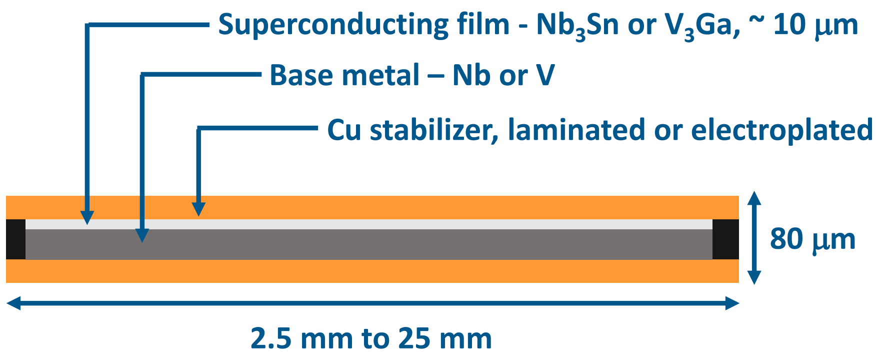

M. G. Benz, IEEE Trans. Mag. 2 (1966) 760

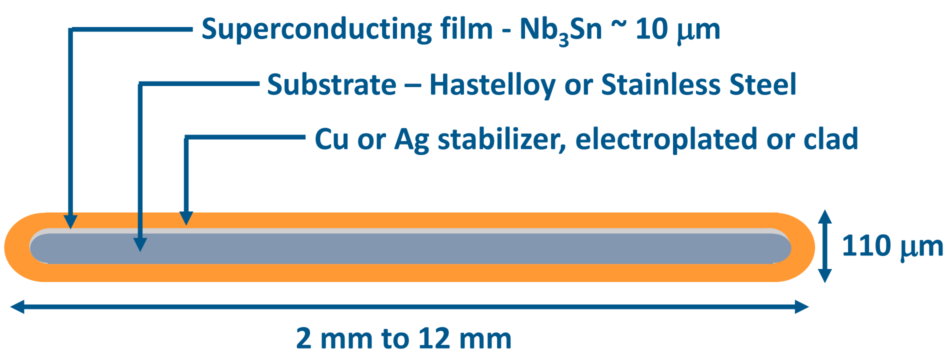

J. Hanak, US Pat. 3420707A (Filed Dec. 28, 1964)

Liquid Diffusion Process

Nb ribbon coated with Sn and heat treated at 900-1200°C for several hours

Developed at General Electric and used in 15 T-class R&W magnets

Vapor Deposition Process

A metallic substrate heated at 1200°C and traveling in a reaction chamber with a flow of gaseous $NbCl_4$, $SnCl_2$, H_2 and He

Developed at RCA

A similar process is used for producing SRF cavities for accelerators based on Nb_3Sn

S. Posen and D. L . Hall, SUST 30 (2017) 033004

1966-1969: A small addition of Cu…

The Bronze Process and the development of multifilamentary wires

K. Tachikawa and his co-workers at NRIM, Tokyo, developed V_3Ga tapes with very high in-field current by the liquid diffusion process

Tachikawa discovered that Cu was acting as a catalyst for the formation of the A15 phase, making possible the synthesis of V_3Ga at lower temperatures

K. Tachikawa, Y. Tanaka and S. Fukuda, Japan Pat. 0670619 (Filed June 25, 1966)

K. Tachikawa and Y. Tanaka, Jap. J. Applied Physics 6 (1967) 782

Prof. Kyoji TACHIKAWA

Researcher in UK and US came at the same conclusion almost at the same time

The addition of Cu lowers also the formation temperature of Nb_3Sn from above 930°C to more practical values of ~650°C

The idea was extended to the formation of Nb_3Sn by solid state diffusion at the interface of Nb and Cu-Sn alloy (bronze). This principle was used for the development of the first multifilamentary Nb_3Sn wires

The Bronze Process for multifilamentary Nb_3Sn wires

E. W. Howlett, Great Britain Pat. 52, 623/69 (Filed Oct. 27, 1969)
A. R. Kaufman and J. J. Pickett, Bull. Am. Phys. Soc. 15 (1970) 833

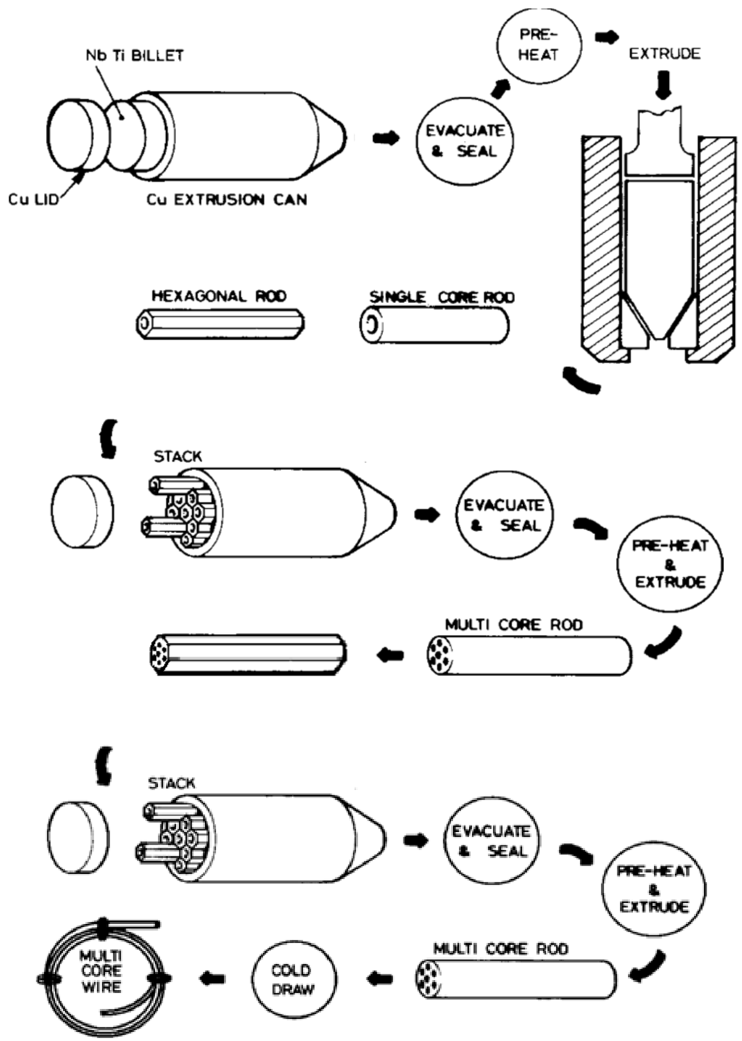

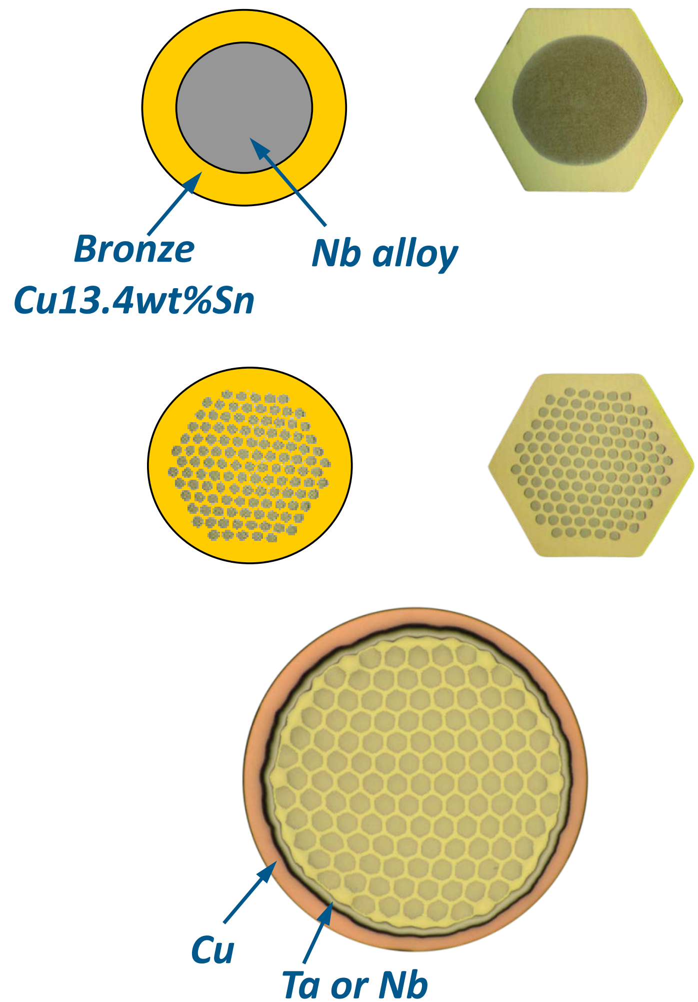

Industrial fabrication of multifilamentary Nb_3Sn wires

Three technologies developed at industrial scale

The main difference comes from the type of Sn source

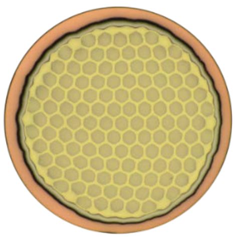

Bronze Process

Bronze is the Sn source, limited by the solubility of Sn in Cu

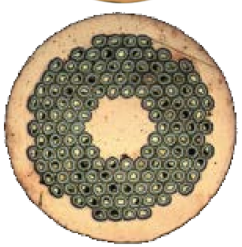

Internal Sn Diffusion Process

A metallic Sn rod is inserted in the subelement core

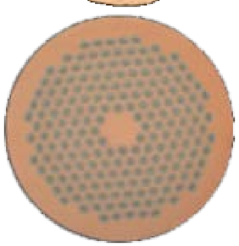

Powder-In-Tube (PIT) method

Each subelement is a Nb-alloy tube filled with $NbSn_2$ and Sn powders

Presently produced by BRUKER, LUVATA, Western Superconducting Technologies Co.,Ltd., Bochvar Institute of Inorganic Materials JSC VNIINM, Kiswire, FURUKAWA ELECTRIC, JASTEC Superconductor

What controls the performance of Nb_3Sn

- *Influence of Sn composition on T_c and B_{c2}*
- *Doping to further enhance B_{c2}*
- *Grain boundaries and vortex pinning*

Influence of the Sn composition of T_c and B_{c2}

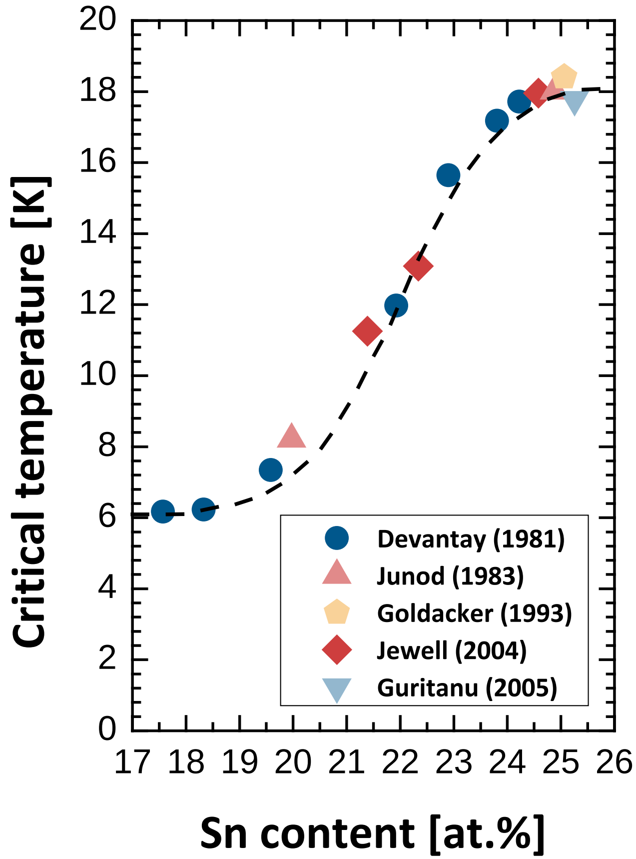

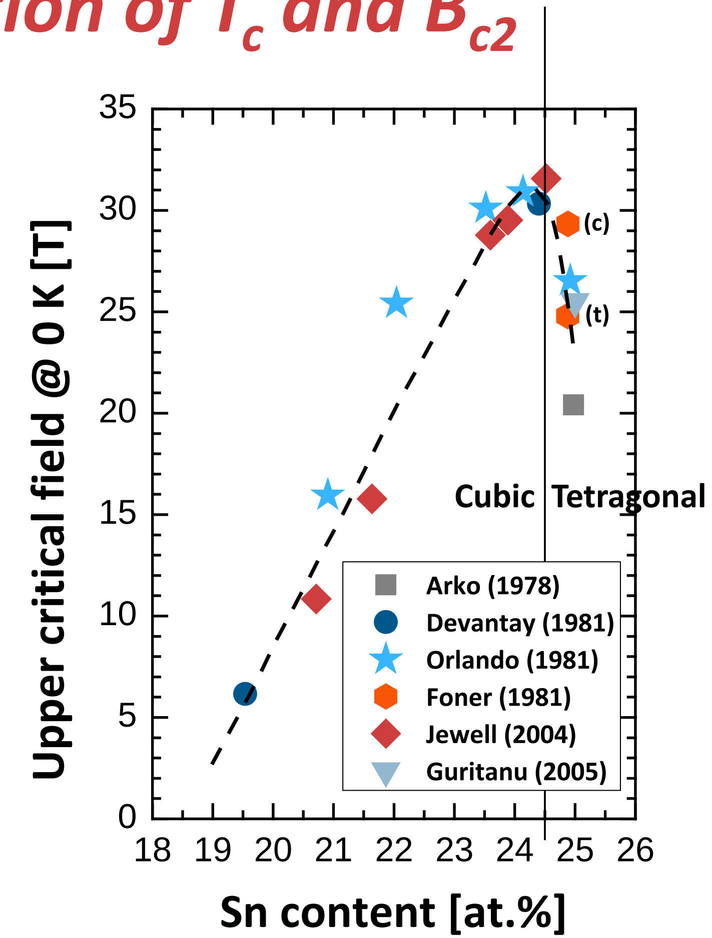

Adapted from R. Flükiger et al., Cryogenics 48 (2008) 293

$Nb_{3+x}Sn_{1-x}$ is superconducting also when deviates from stoichiometry

$$B_{c2} \propto \gamma \rho_n T_c$$

Doping to further enhance B_{c2}

The additions of Ta and Ti are particularly beneficial

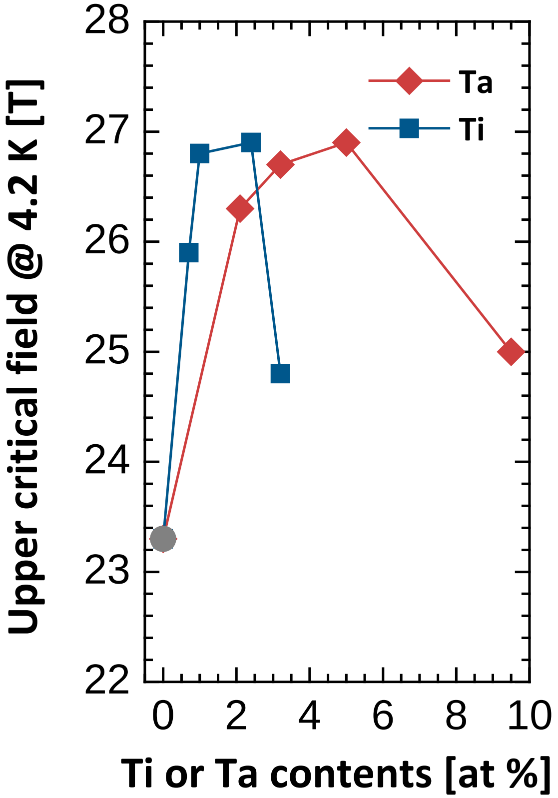

Adapted from M. Suenaga et al., JAP 59 (1986) 840

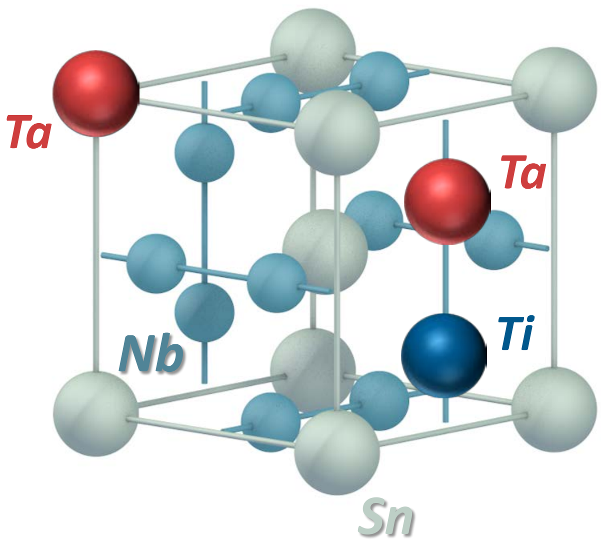

From EXAFS investigations

- *Ti substitutes Nb*
- *Ta substitutes both Nb and Sn*

S. M. Heald et al., Sci. Rep. 8 (2018) 4798

All industrial Nb_3Sn wires are doped either with Ti or with Ta

Vortex pinning at the grain boundaries in Nb_3Sn

Impede vortex motion to increase J_c

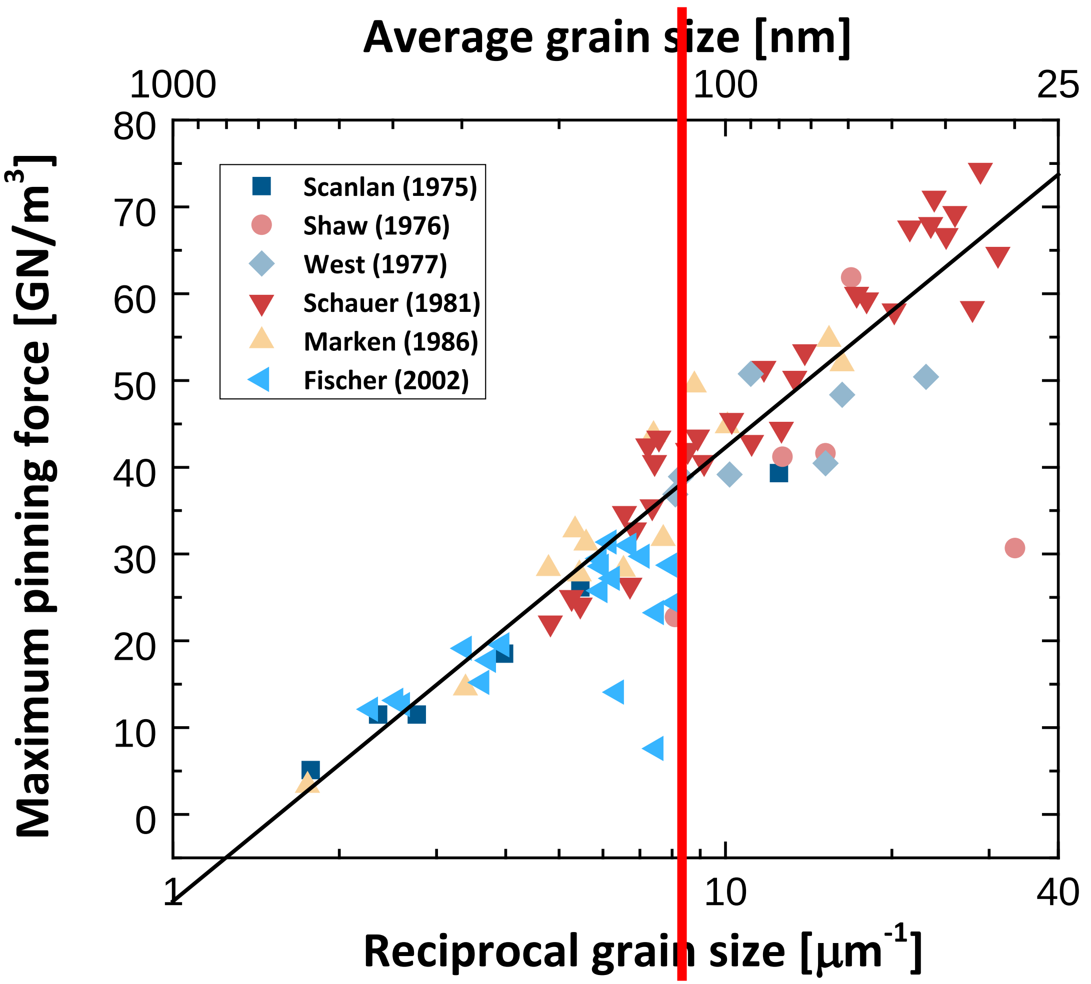

Adapted from A. Godeke, SUST 19 (2006) R68

Composition and microstructure in industrial wires

Bronze

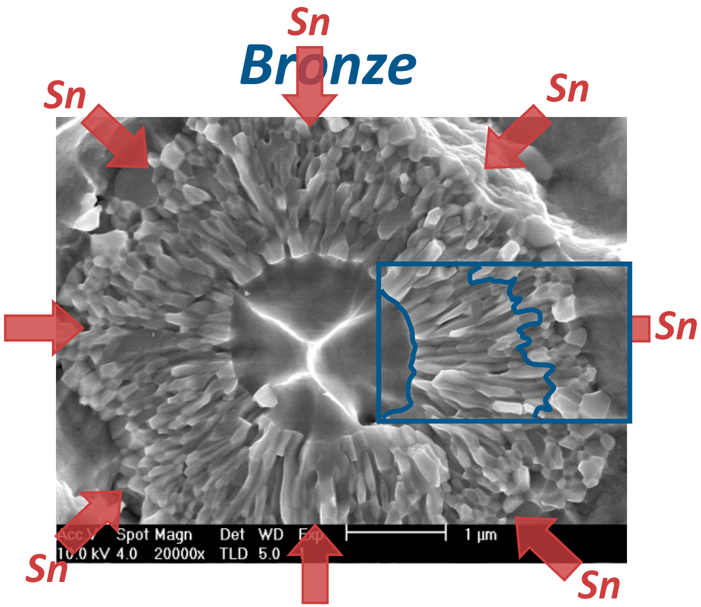

Filament size ~5 µm

Outer region

Equiaxed grains ~ 150 nm

Composition 21-25 at.% Sn

Inner region

Columnar grains ~ 400 nm

Composition 18-21 at.% Sn

Internal Sn

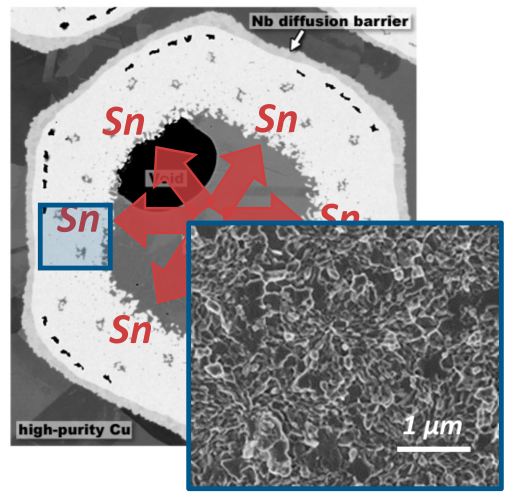

Subelement size ~50 µm

Almost everywhere

Fine grains ~ 100-150 nm

Composition 23-25 at.% Sn

Powder-In-Tube

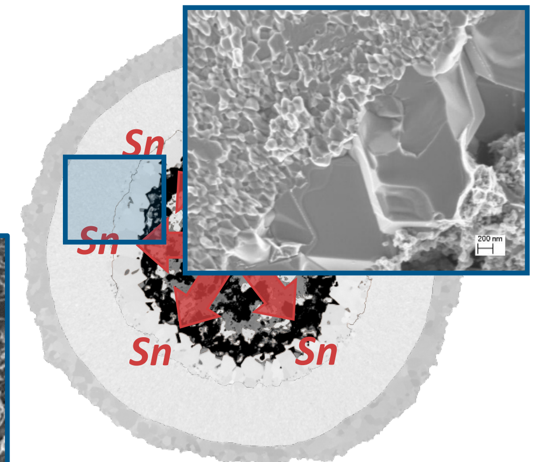

Subelement size ~50 µm

Outer region

Fine grains ~ 150 nm

Composition 23-24 at.% Sn

Inner region

Large grains ~ 1 µm

Composition 25 at.% Sn

Composition and microstructure in industrial wires

Bronze

Filament size ~5 µm

Outer region
Equiaxed grains ~ 150 nm
Composition 21-25 at.% Sn

Inner region
Columnar grains ~ 400 nm
Composition 18-21 at.% Sn

Internal Sn

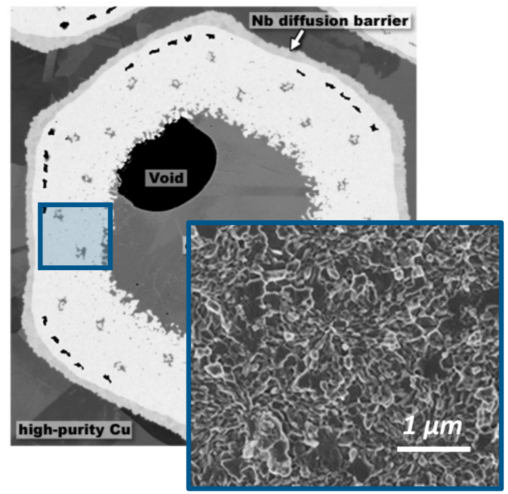

Subelement size ~50 µm

Almost everywhere
Fine grains ~ 100-150 nm
Composition 23-25 at.% Sn

Powder-In-Tube

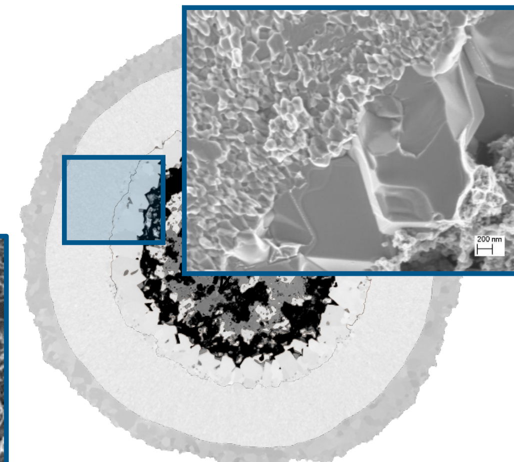

Subelement size ~50 µm

Outer region
Fine grains ~ 150 nm
Composition 23-24 at.% Sn

Inner region
Large grains ~ 1 µm
Composition 25 at.% Sn

High performance Nb_3Sn wires

Outline

A brief introduction to A15 superconductors

Nb_3Sn: the pathway to industrialization

Towards the ultimate performance of Nb_3Sn

- ***the Future Circular Collider study @ CERN***

Not only critical current !!

- *Focus on the electromechanical properties*

The Future Circular Collider Study

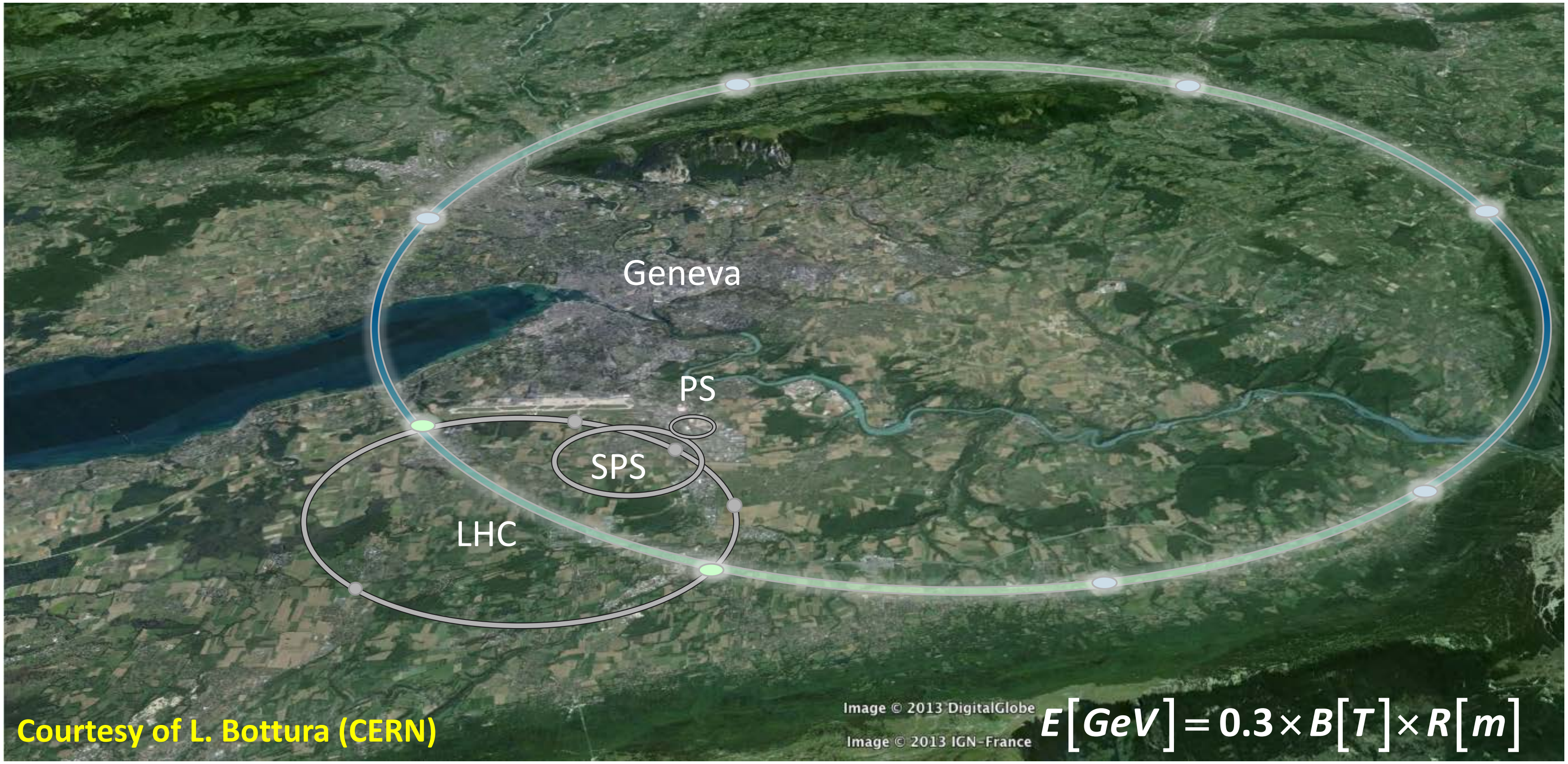

$$E[GeV] = 0.3 \times B[T] \times R[m]$$

LHC	FCC-hh
27 km, 8.33 T	100 km, 16 T
14 TeV (c.o.m.)	100 TeV (c.o.m.)
1300 tons NbTi	~9000 tons Nb_3Sn

Performance target for the 16 T FCC dipoles

non-Cu J_c(4.2 K,16 T) = 1'500 A/mm^2

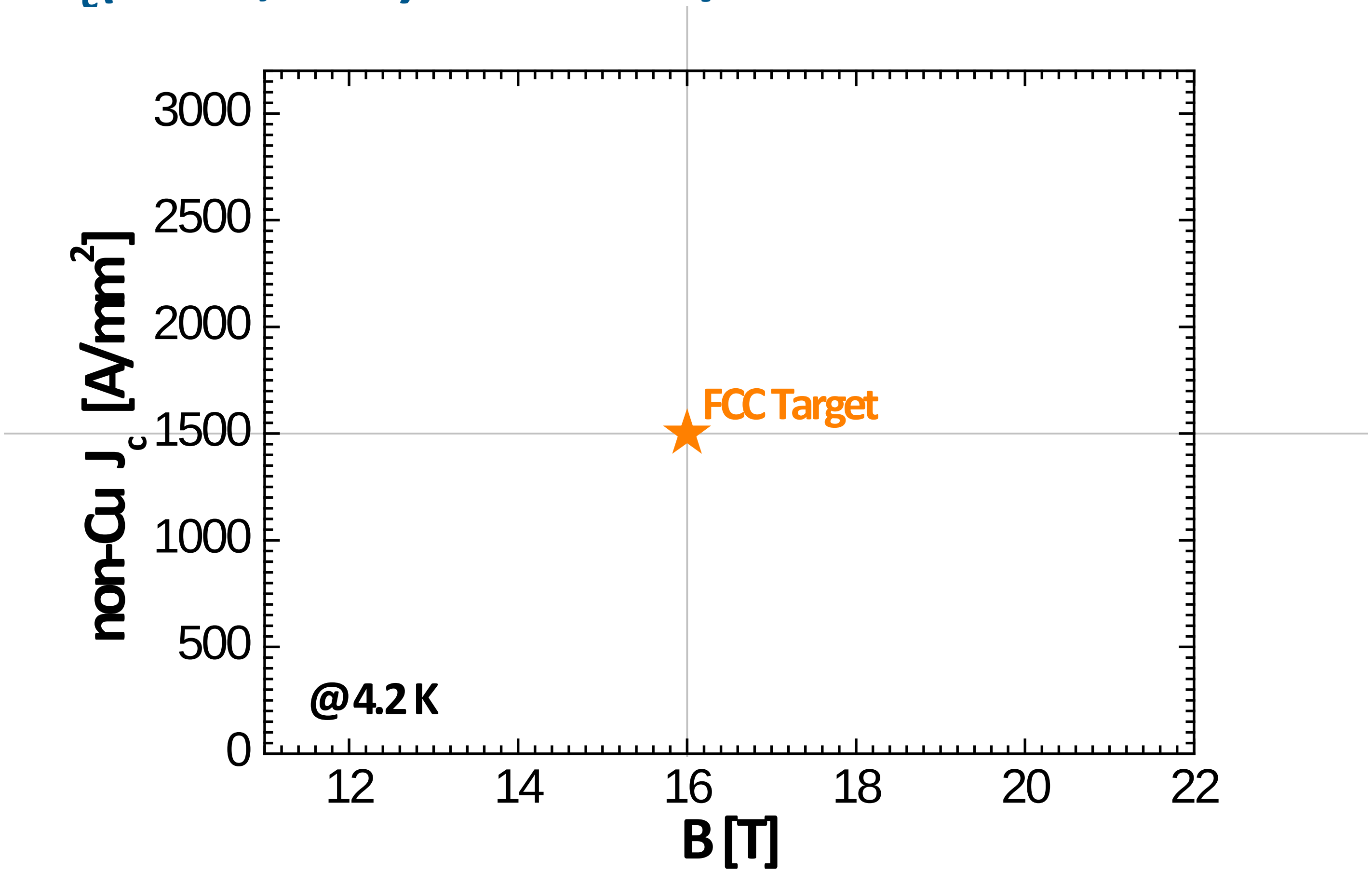

Performance target for the 16 T FCC dipoles

non-Cu J_c(4.2 K,16 T) = 1'500 A/mm²

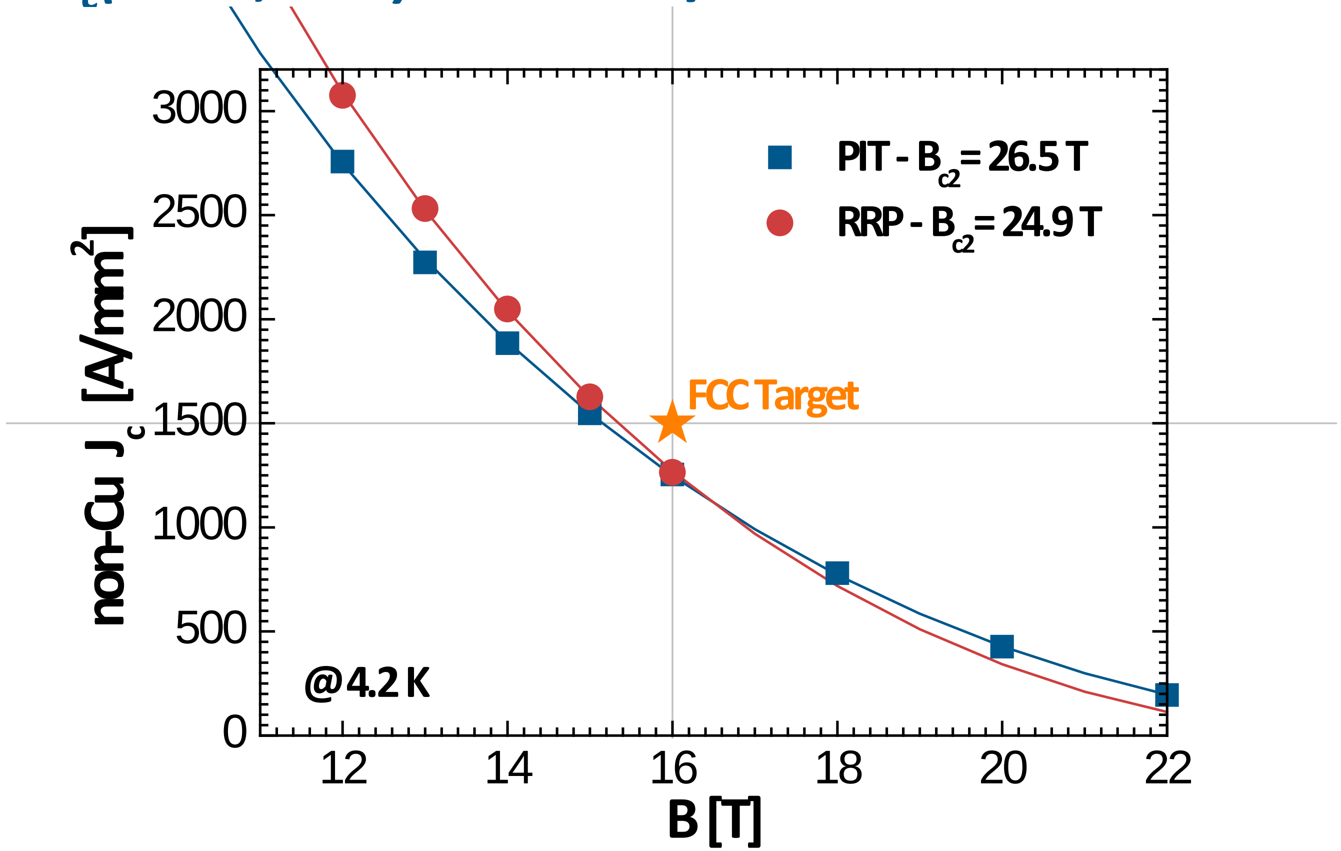

J. Parrell et al., AIP Conf. Proc. 711 (2004) 369

T. Boutboul et al., IEEE TASC 19 (2009) 2564

Strategies to increase the in-field critical current density
= to enhance the pinning at high field

Increase the grain boundary density
i.e. refine the grain size

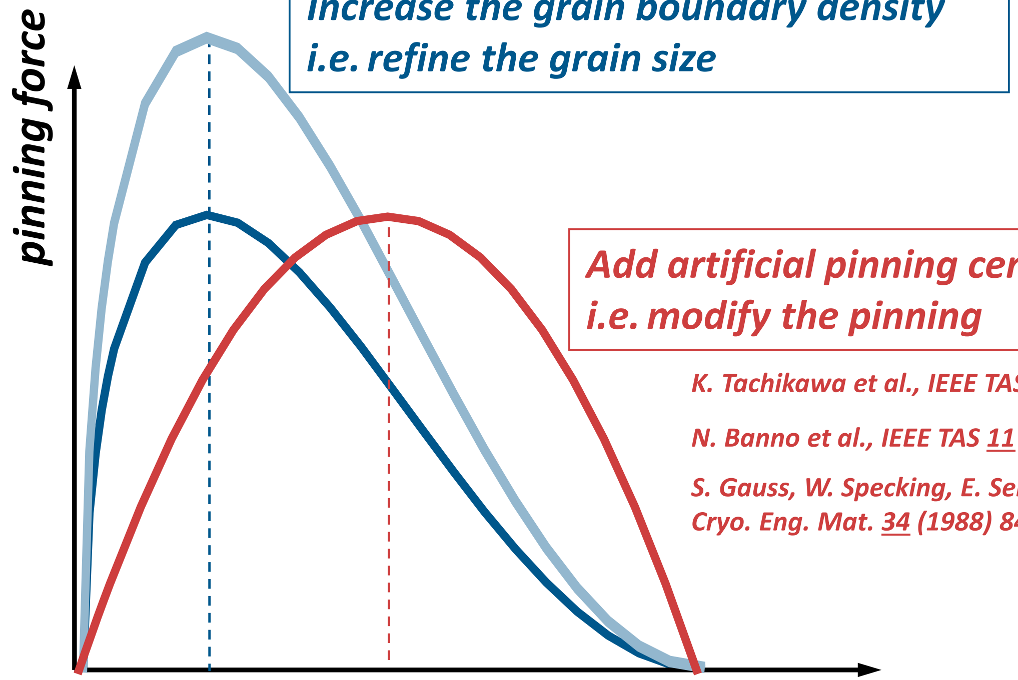

Add artificial pinning centers
i.e. modify the pinning

K. Tachikawa et al., IEEE TAS 13 (2003) 3438

N. Banno et al., IEEE TAS 11 (2001) 3696

S. Gauss, W. Specking, E. Seibt and R. Flükiger, Adv. Cryo. Eng. Mat. 34 (1988) 843

max at B = 0.2 B_{c2}
Grain boundary pinning

max at B = 0.33 B_{c2}
Point-like pinning

… but how to obtain grain refinement ?

Grain refinement by Internal Oxidation in Nb_3Sn

Idea from Benz (1968) to form fine precipitates in Nb to impede the Nb_3Sn grain growth

M. G. Benz, Trans. Metall. Soc. AIME, 242 (1968) 1067-1070

Use of a Nb-Zr alloy: Zr has stronger affinity to oxygen than Nb

THE OHIO STATE UNIVERSITY

Oxygen supply added to the composite: oxidation of Zr and formation of nano-ZrO_2

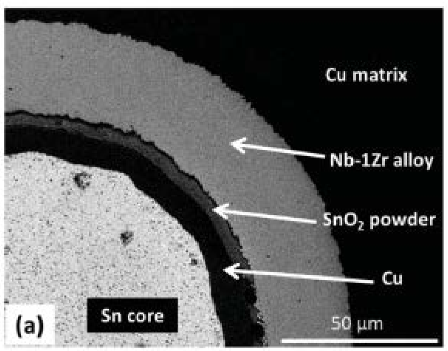

X. Xu et al., APL 104 (2014) 082602
X. Xu et al., Adv. Mat. 27 (2015) 1346

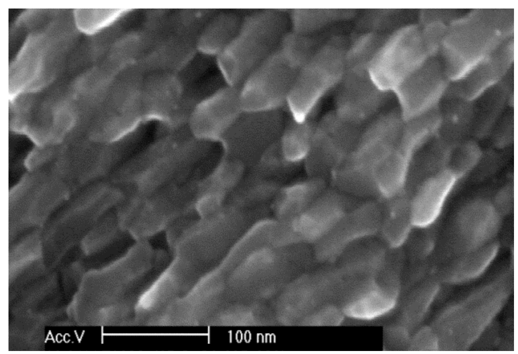

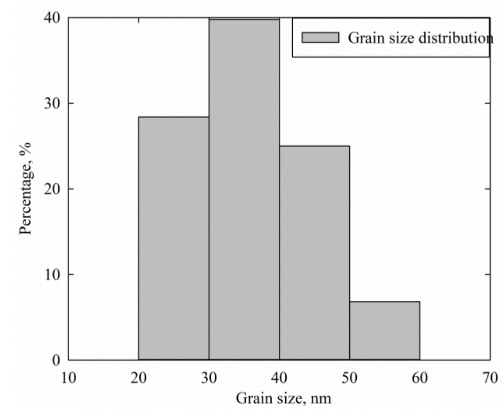

Average grain size is reduced down to ~ 50 nm in binary Nb_3Sn

Recent advances on Ta-doped Nb_3Sn

48 filaments, Zr addition, grain size 70-80 nm
X. Xu et al., SuST 32 (2019) 02LT01

monofilaments, Hf addition, grain size 50-70 nm
grain refinement without additional oxygen source
S. Balachandran et al., SuST 32 (2019) 044006

Performance target non-Cu $J_c(4.2K,16\ T) = 1500\ A/mm^2$

First report on a wire hitting the FCC specs

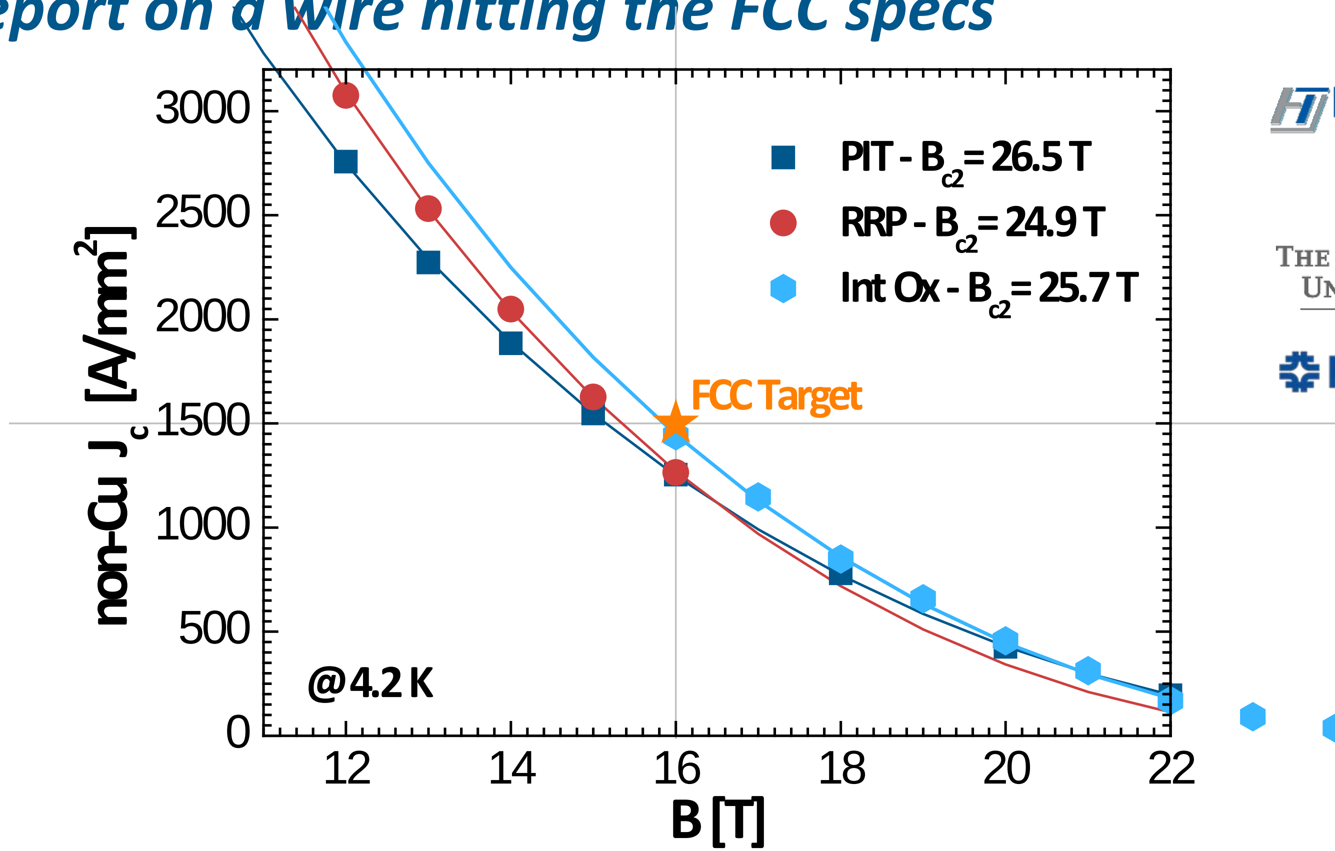

Hyper Tech

The Ohio State University

Fermilab

X. Xu et al., arXiv 1903.08121 (2019)

J. Parrell et al., AIP Conf. Proc. 711 (2004) 369

T. Boutboul et al., IEEE TASC 19 (2009) 2564

Advances on Internal Oxidation at UNIVERSITÉ DE GENÈVE FACULTÉ DES SCIENCES

Activity funded in the frame of a FCC collaboration with CERN

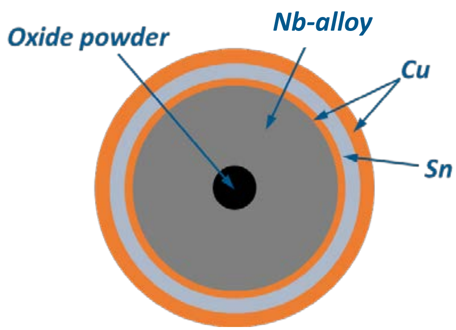

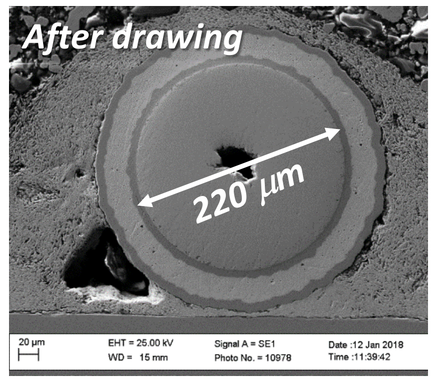

Nb-alloy
Nb-7.5wt%Ta (REF.)
Nb-1wt%Zr
Nb-7.5wt%Ta-1wt%Zr
Nb-7.5wt%Ta-2wt%Zr

Ø 220 μm wires of Nb-alloy were prepared by cold deformation of Ø 12 mm rod with nano-sized powders compacted in a central hole

Nb alloy wire was then electroplated successively with: Cu, Sn, Cu

Evaluated SnO_2 and CuO as oxygen sources, for these reasons

- *high Gibbs free energy of formation*
- *low hardness that would make it compatible with wire fabrication*
- *the metal resulting from the reduction not affecting superconductivity*

Florin BUTA et al., @EUCAS 2019

Grain morphology of Nb_3Sn

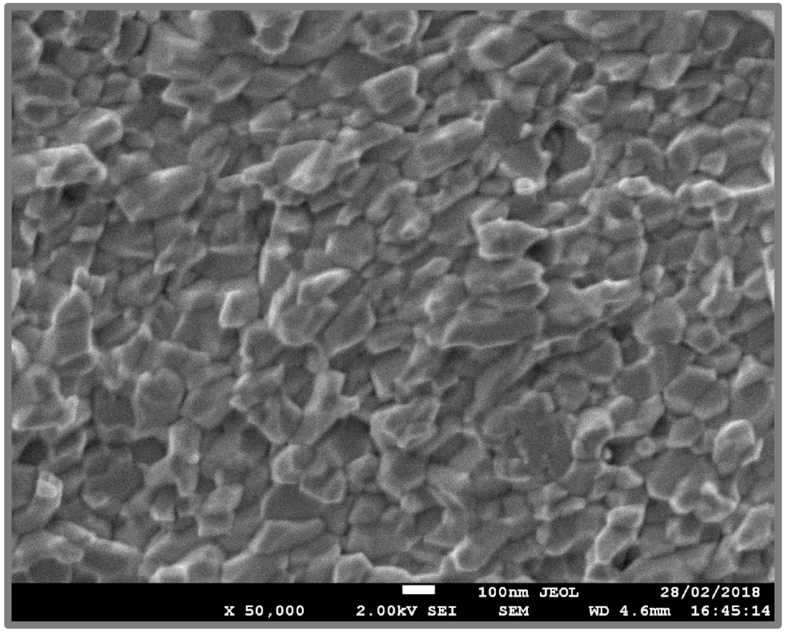

Starting alloy: Nb7.5Ta
no oxygen source
HT: 650°C/200h

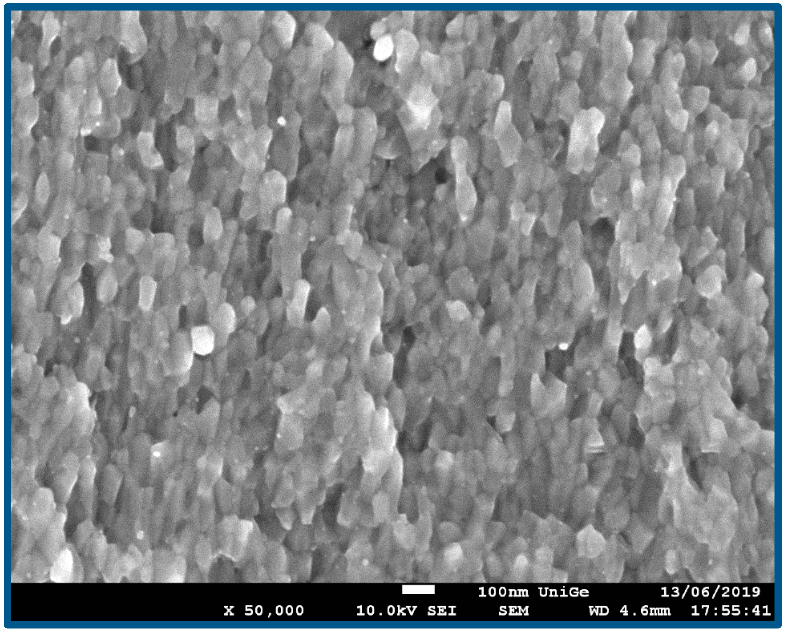

Starting alloy: Nb7.5Ta2Zr
oxygen source: SnO_2
HT: 650°C/200h

Significantly smaller grains in the samples based on Zr alloys and oxygen source

Elongated grains

Grain size distribution

Grain size distribution in the short axis direction

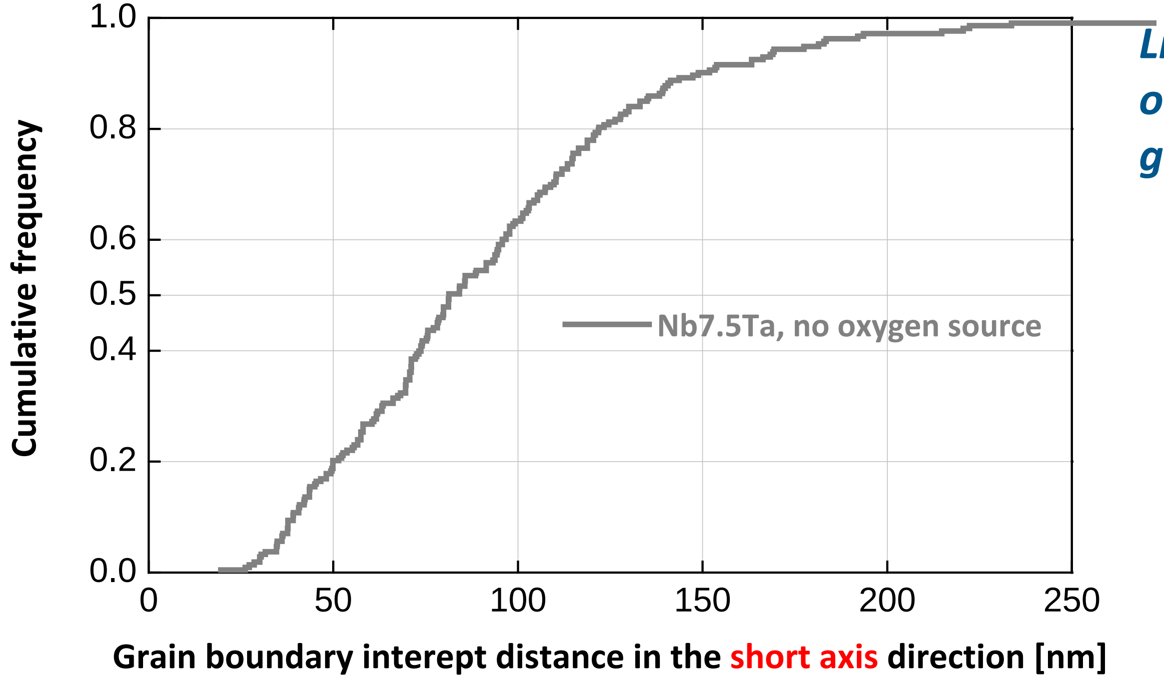

Linear intercept method used to obtain information regarding the grain size distribution

Grain size distribution

Grain size distribution in the short axis direction

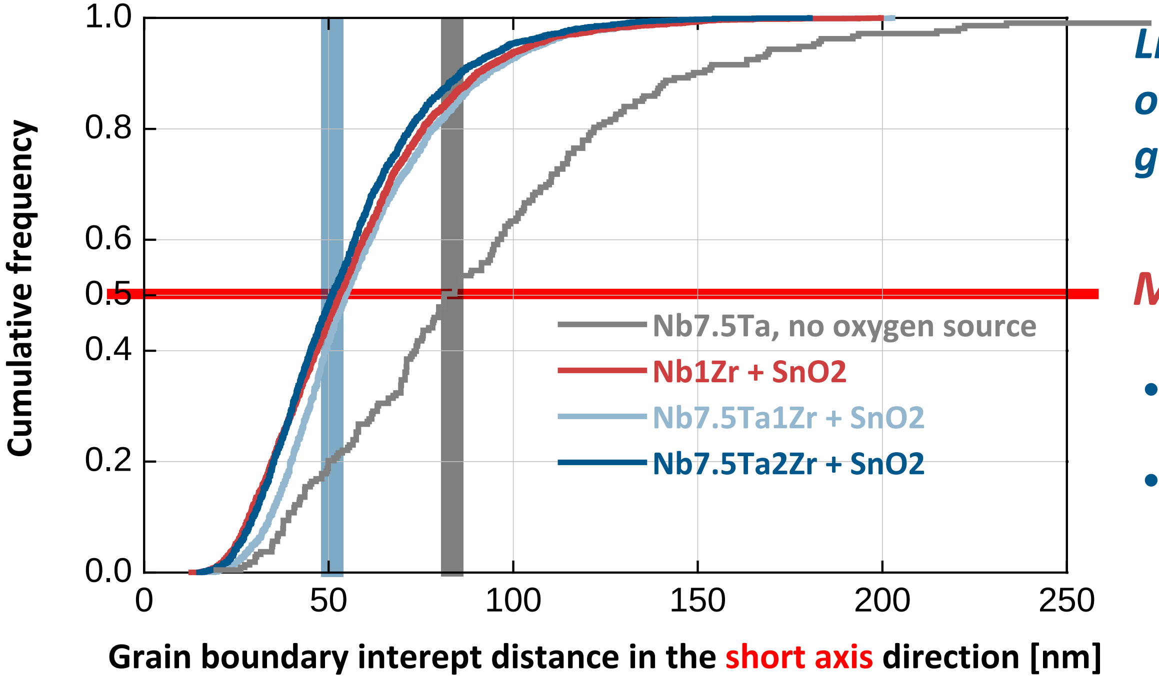

Linear intercept method used to obtain information regarding the grain size distribution

Median sizes

- *Nb7.5Ta based samples ~80 nm*
- *Zr containing samples ~50 nm*

In the long axis direction the median grain size decreases from ~120 nm down to ~85 nm

Critical current density and pinning

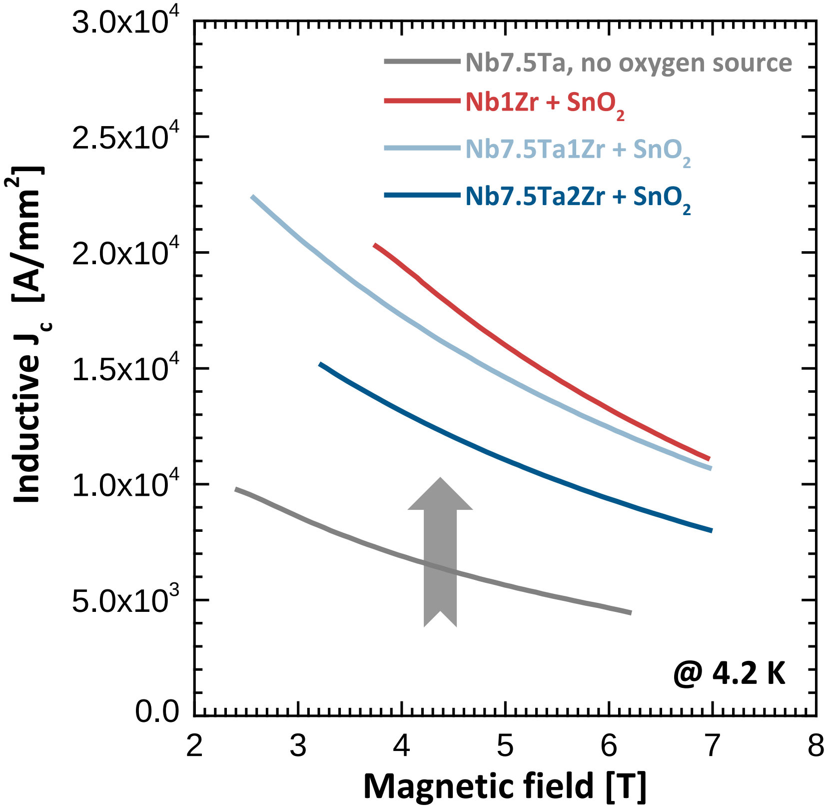

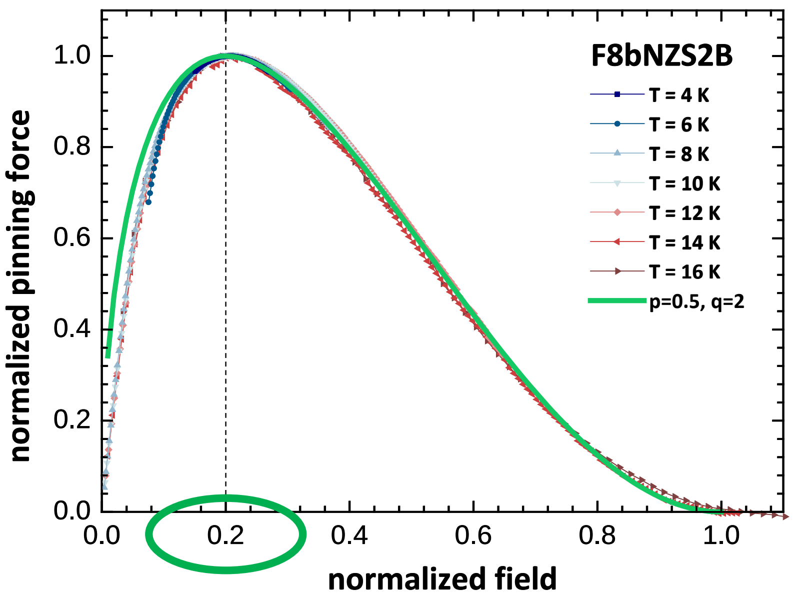

The maximum of f_p stays close to 0.2 for all our samples, regardless of alloy, Zr content and oxygen source.

The critical current density is strongly enhanced in the presence of Zr and O

The main vortex pinning mechanism remains the same: grain boundary pinning

Upper critical fields at 4.2 K

Critical fields from R(B) performed at LNCMI Grenoble under magnetic fields up to 33 T

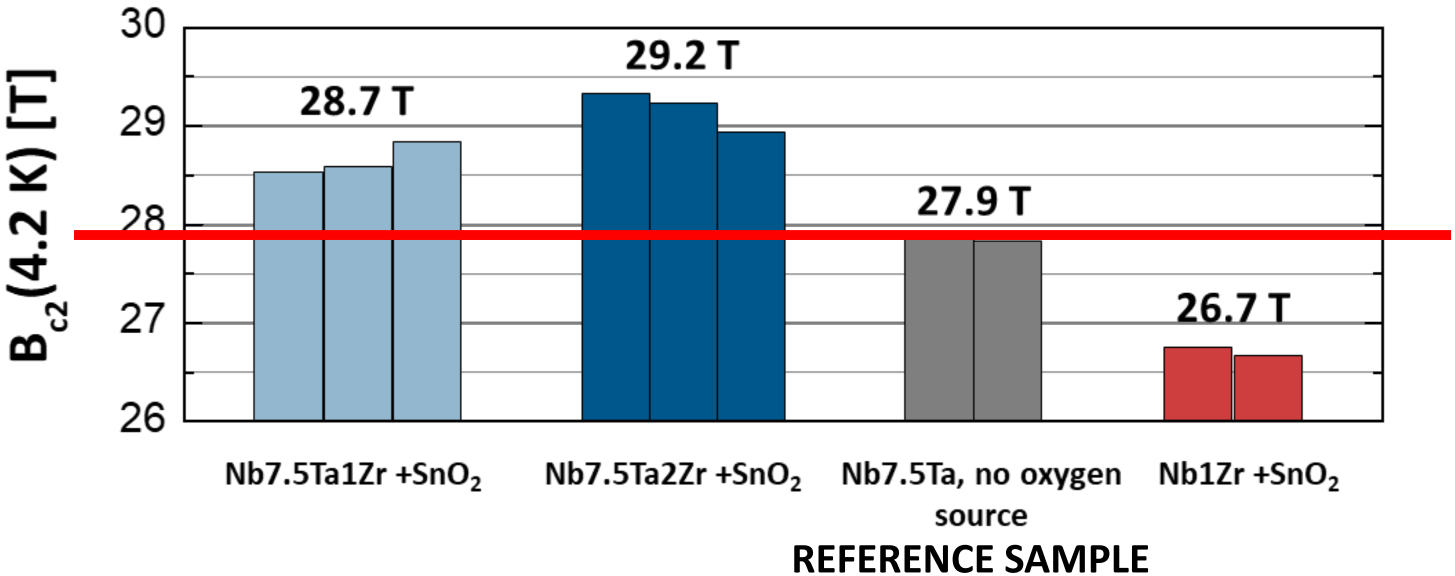

The combined presence of Ta and Zr further increases the upper critical field up to ~ 29 T , i.e. to higher values than obtained for Nb7.5Ta

This is showing that it is possible to further improve the field performance of Nb_3Sn wires

Outline

A brief introduction to A15 superconductors

Nb_3Sn: the pathway to industrialization

Towards the ultimate performance of Nb_3Sn

- *the Future Circular Collider study @*

Not only critical current !!

- ***Focus on the electromechanical properties***

Electromagnetic forces in a magnet

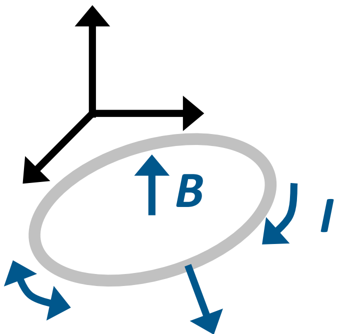

$$\sigma_{hoop} = \frac{I}{S_{wire}} BR$$

$$F = I \times B$$

Hoop stress levels well above 100 MPa are common

Stress increases proportionally to field, current density and magnet size

In real magnets conductors are exposed to 3D stresses that combine axial tension and transverse compression

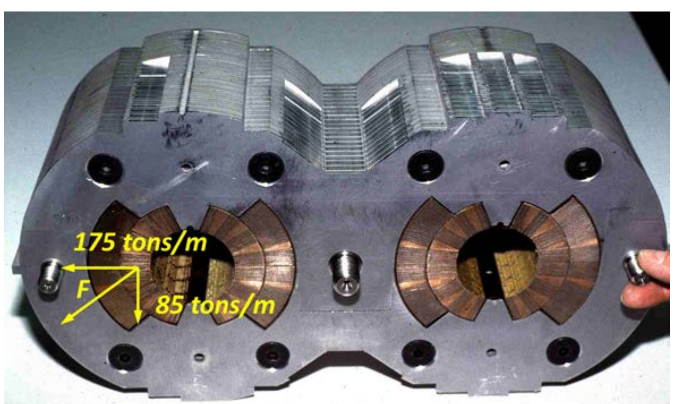

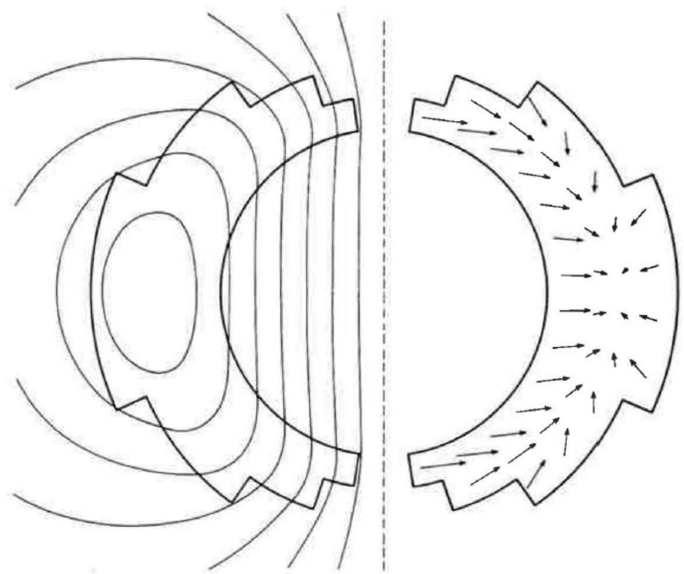

magnetic lines of force

vectors of electromagnetic force per unit volume

Strain-induced changes in the critical current of Nb_3Sn wires

Effects of the axial strain

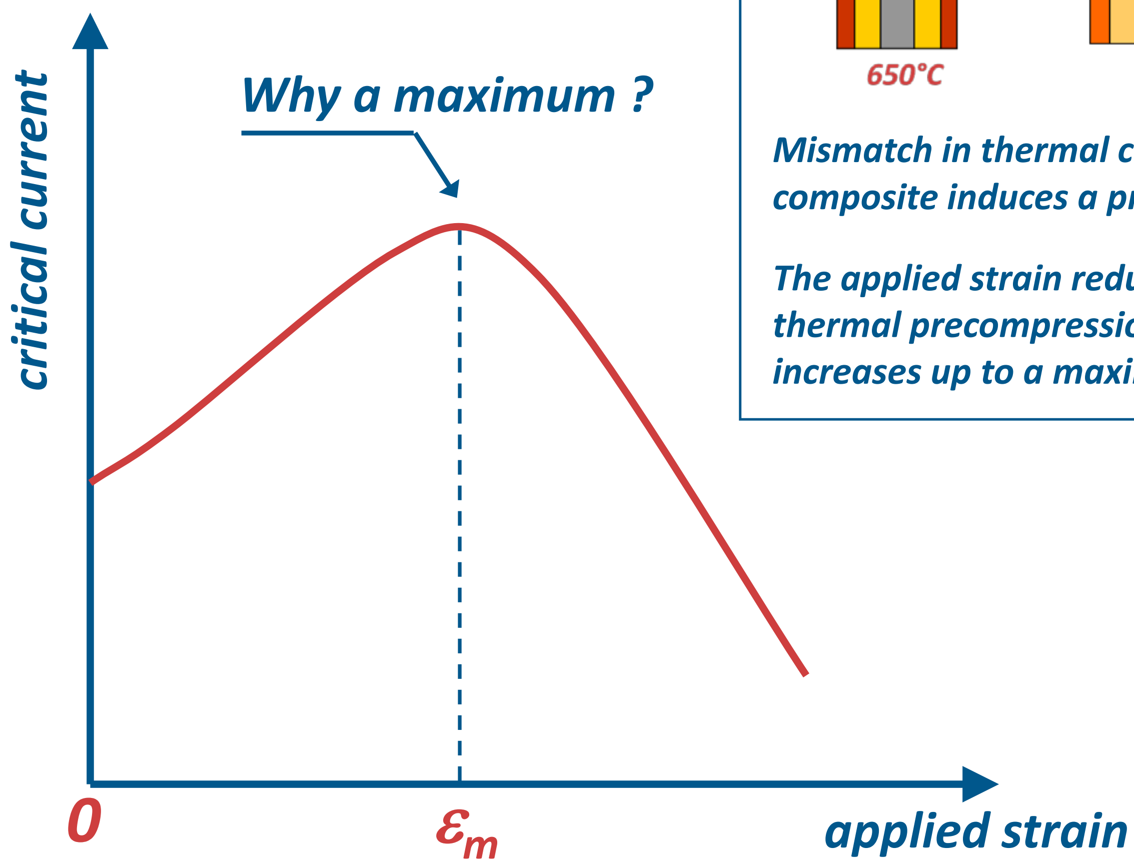

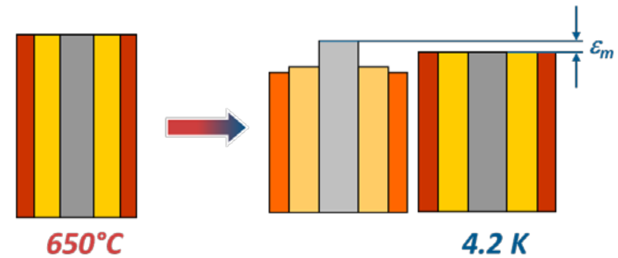

Mismatch in thermal contraction within the composite induces a precompression in Nb_3Sn

The applied strain reduces the effects of the thermal precompression and the critical current increases up to a maximum

Lattice parameters and I_c under axial strain

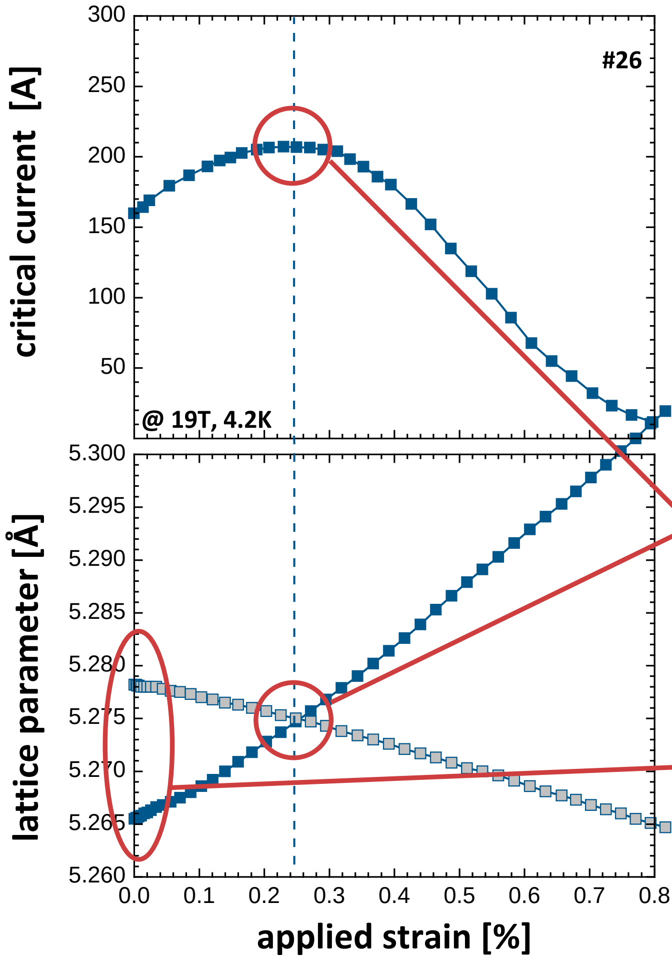

IOP Publishing — Superconductor Science and Technology
Supercond. Sci. Technol. 28 (2015) 045016 (9pp) — doi:10.1088/0953-2048/28/4/045016

Local strain exerted on Nb_3Sn filaments in an ITER strand

K. Osamura et al.

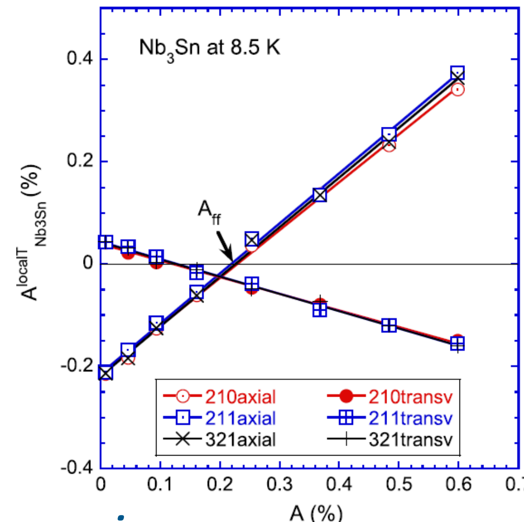

CROSSING POINT
Cubic cell recovered

This corresponds to the maximum of the critical current

ZERO APPLIED STRAIN
Nb_3Sn is precompressed
The cell is distorted

Tests on a Bronze Route wire

XRD experiments @ ESRF

C. Scheuerlein et al., IEEE TASC 19 (2009) 2653
L. Muzzi et al., SUST 25 (2012) 054006

Prebending to remove the precompression

CuNb-reinforced Nb_3Sn wires for the 25 T cryogen-free magnet @ TOHOKU UNIVERSITY

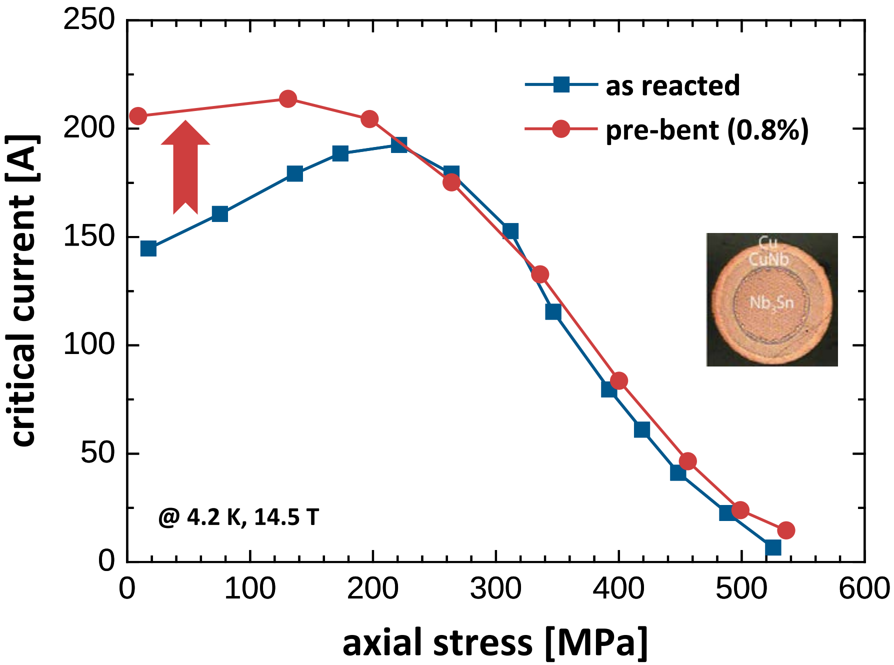

Adapted from H. Oguro et al., IEEE TASC 24 (2014) 8401004

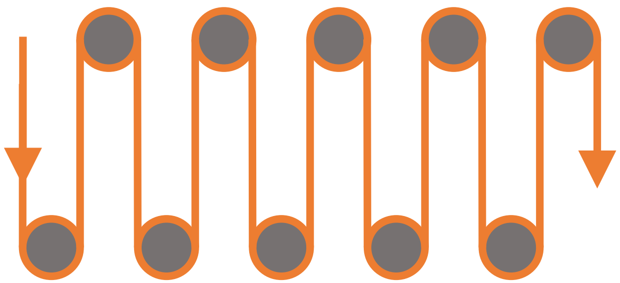

Repeated bending at room temperature after the reaction heat treatment

The prebending leads to a precompression release in Nb_3Sn through the plastic deformation of CuNb $\Rightarrow$ significant improvement of I_c at low applied stress

Strain-induced changes in the critical current of Nb_3Sn wires

Effects of the axial strain

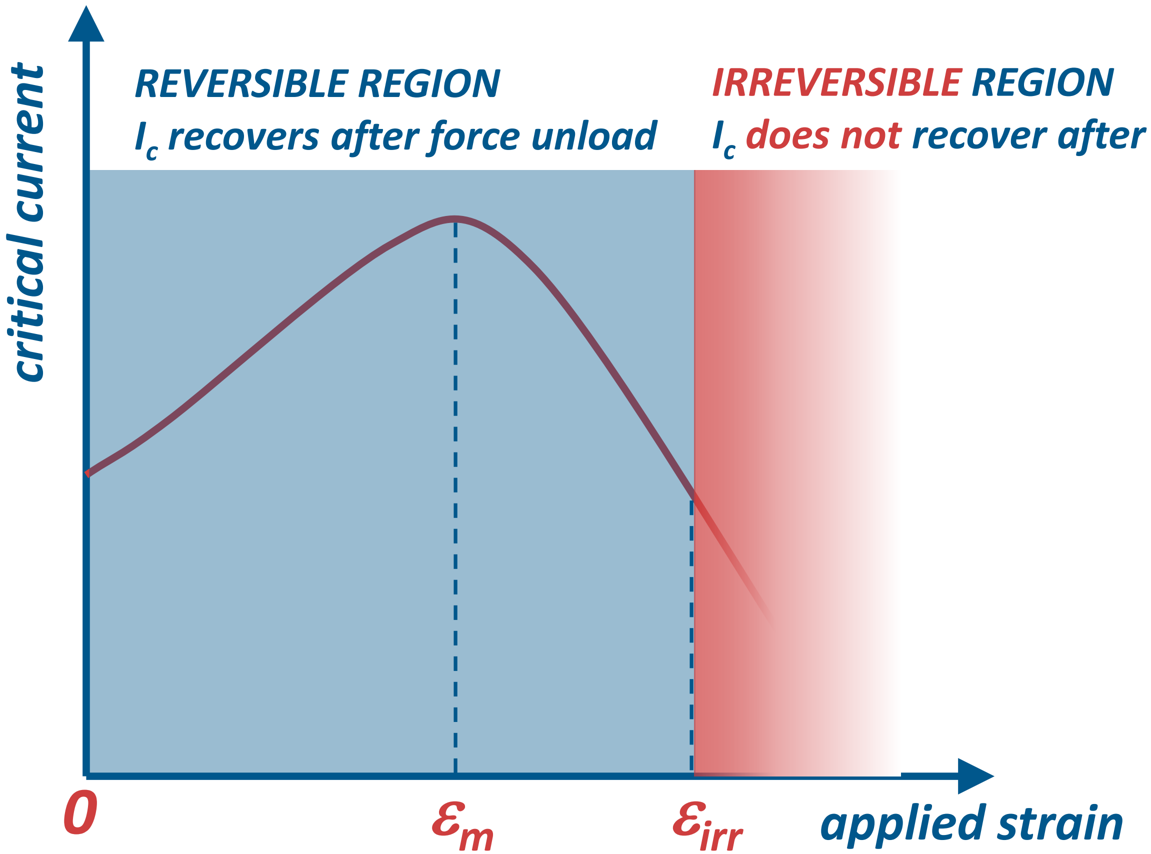

Irreversible degradation phenomena

Two mechanisms govern the irreversible degradation of the critical current

- ***Formation of cracks in the Nb_3Sn filaments due, for instance, to the stress concentration at the voids formed during the reaction heat treatment***

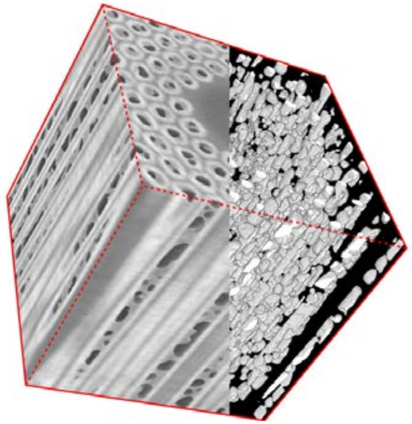

- ***Plastic deformation of the matrix and residual stress on the Nb_3Sn filaments.***

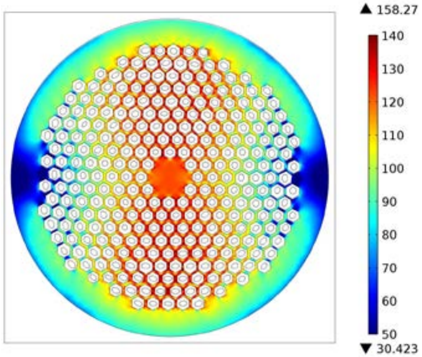

Which mechanism dominates the irreversible degradation of the critical current ?

Analysis of the phenomenon in two load geometries

1 – Axial tension and the role of cracks at the voids

2 – Transverse compression, plastic deformation of the matrix and residual stress on Nb_3Sn

Analysis of the phenomenon in two load geometries

1 – Axial tension and the role of cracks at the voids

2 – Transverse compression, plastic deformation of the matrix and residual stress on Nb_3Sn

Voids detection in Nb_3Sn wires

X-ray microtomography reconstruction @ ESRF Grenoble

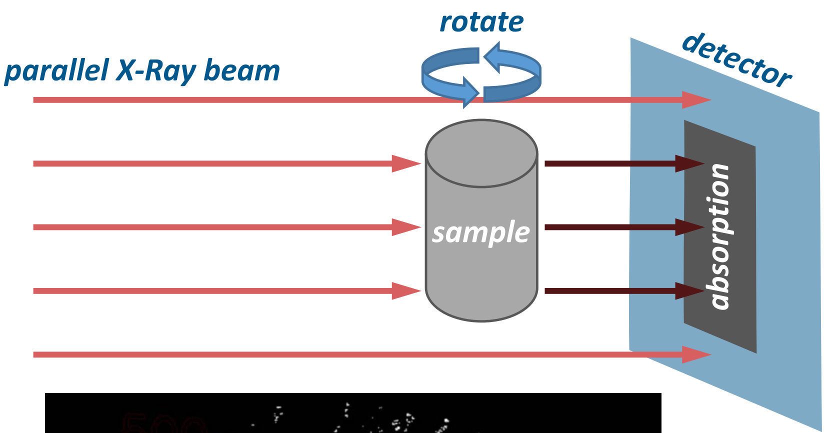

- *X-ray photon energy = 89 keV*
- *360° rotation of the sample*
- *30'000 projections*
- *2560 x 2160 pixels*
- *0.57 μm/pixel resolution*

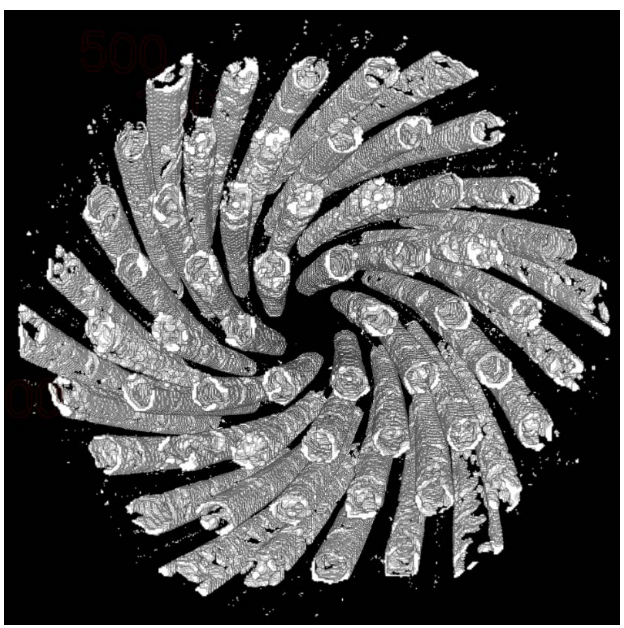

Non-destructive
3D volume reconstruction
with separation of internal features

C. Barth et al., Sci. Rep. 8 (2018) 6589

A case study on Bronze Nb_3Sn wires

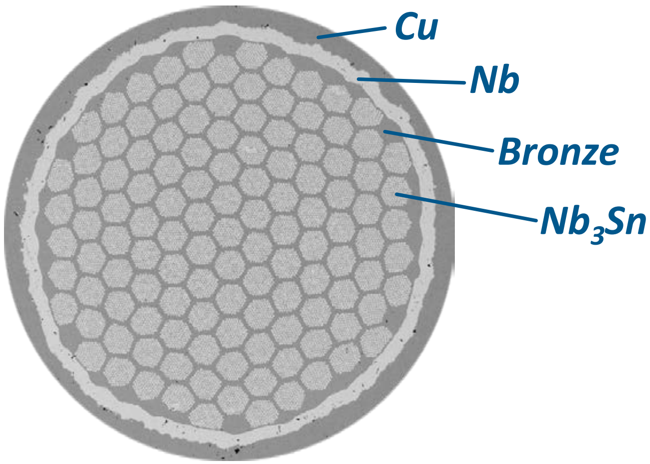

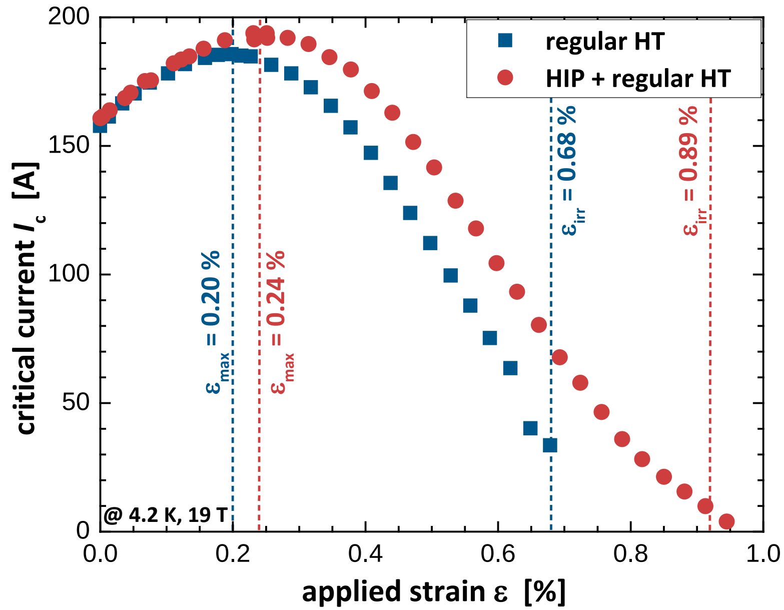

manufacturer	UNIVERSITÉ DE GENÈVE FACULTÉ DES SCIENCES
wire diameter	*1.25 mm*
# of filaments	*121 x 121*
filament size	*4.5 µm*

Regular HT: 600°C/100h + 670°/150h

$\varepsilon_c = \varepsilon_{irr} - \varepsilon_{max} = 0.48\ \%$

HIP 550°C/1h/200MPa + Regular HT

$\varepsilon_c = \varepsilon_{irr} - \varepsilon_{max} = 0.65\ \%$

With HIP treatment ε_c increases by +0.17 %

Bronze wire: Void detection

Without HIP treatment
Void fraction = 2.1 %

With HIP treatment
Void fraction = 0.05 %

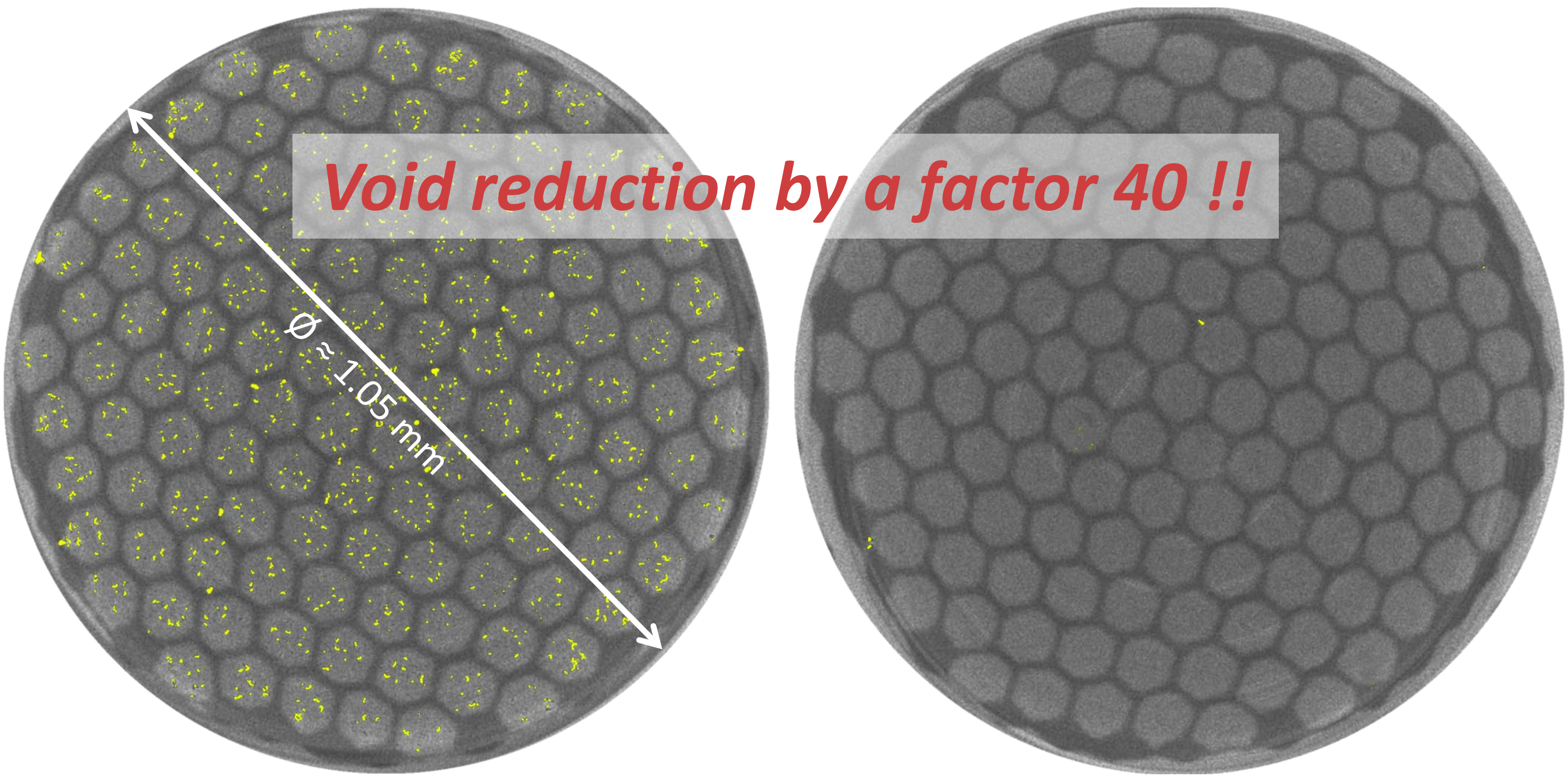

Statistical FEM analysis

- The experimental ε_c corresponds to an irreversible reduction of I_c by 5%
- Working hypothesis: 5% of I_c degradation ≡ damage in 5% of the filaments

Wire without voids

SIMULATION done at ε_c = 0.65%

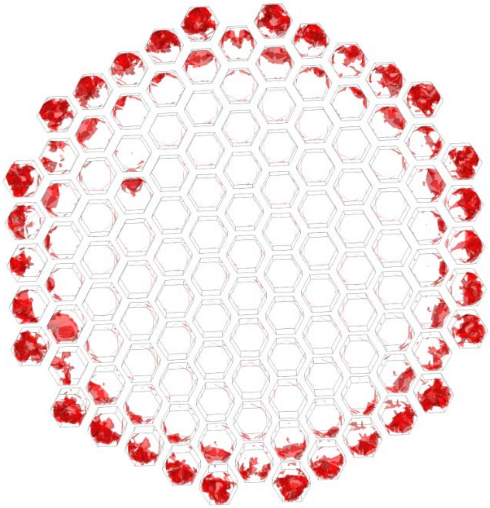

Wire with voids

SIMULATION done at ε_c = 0.50%

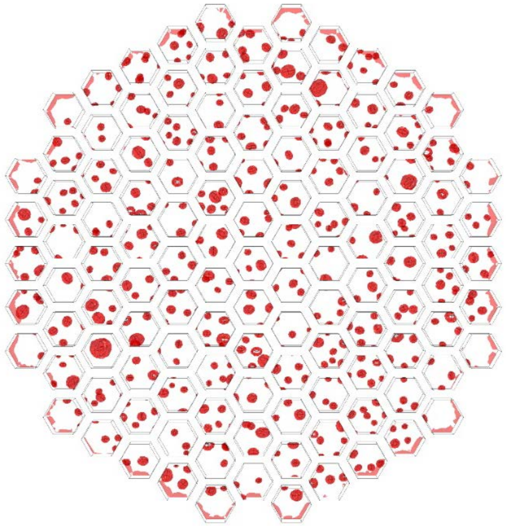

The red regions represent the 5% of the Nb_3Sn volume at the highest stress

Here the red regions are at $\sigma \geq$ 275 MPa, which is the critical stress

Irreversible limit in the presence of voids

Experiment vs Prediction

I_c vs strain measurement

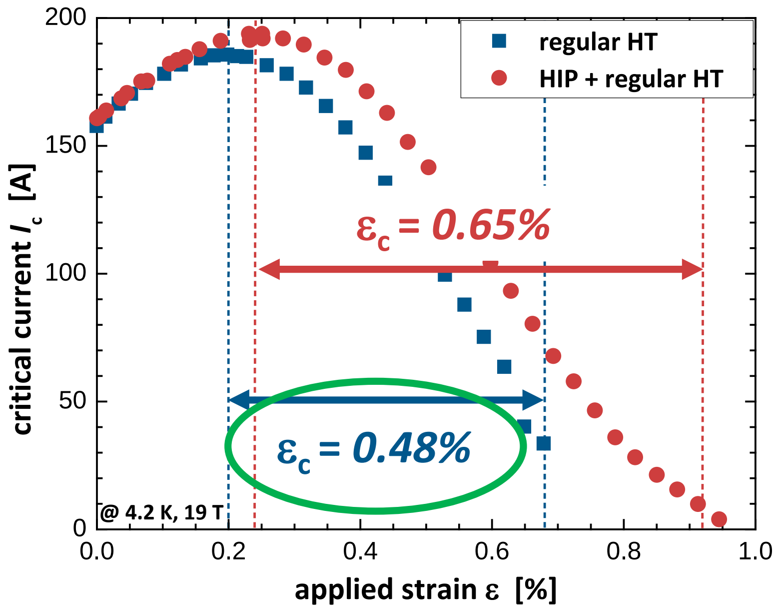

FEM simulations

with voids *without voids*

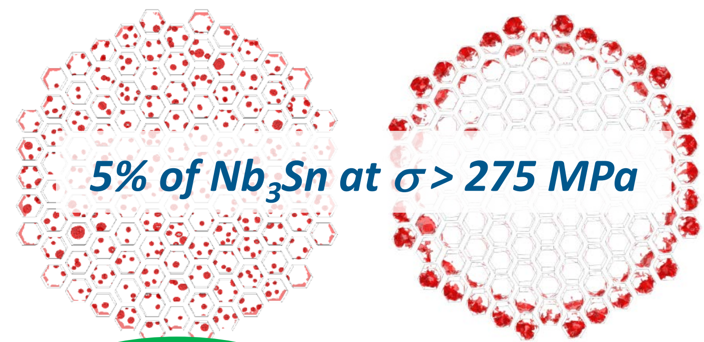

$\varepsilon_c = 0.50\%$ $\varepsilon_c = 0.65\%$

The simulations predict the correct value of ε_c when voids are introduced

Changes in the voids correlate quantitatively with the changes in the electromechanical limits

C. Barth et al., Sci. Rep. 8 (2018) 6589

Analysis of the phenomenon in two load geometries

1 – Axial tension and the role of cracks at the voids

2 – Transverse compression, plastic deformation of the matrix and residual stress on Nb_3Sn

Design options for the 16 T FCC dipoles

h2020 EuroCirCol WP5, started in 2015

WP leader: Davide TOMMASINI, CERN

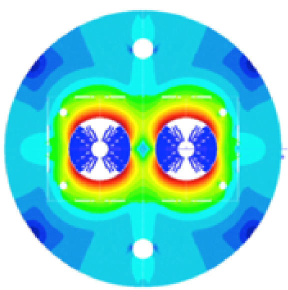

Cosine Theta Coil

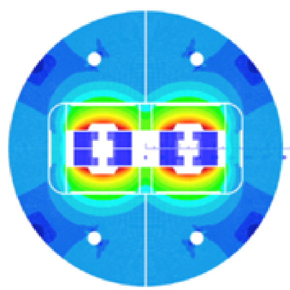

Block Coil

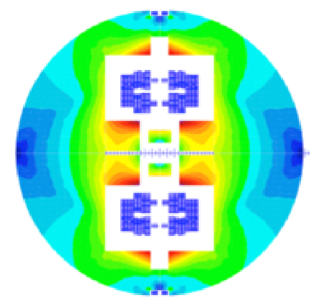

Common Coil

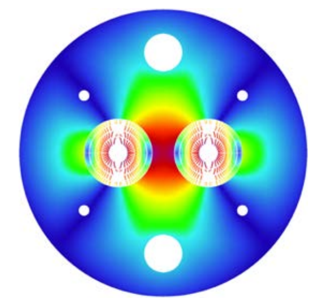

Canted Cosine Theta (CCT)

All designs for the 16 T dipoles share a peak in transverse stress at operation of 150-200 MPa

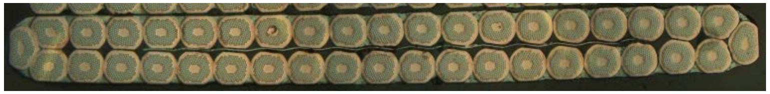

Nb_3Sn Rutherford cable for HL-LHC, 40 strands

Are the Nb_3Sn wires in the Rutherford cables able to withstand such a high stress level? Which degradation is tolerable?

I_c vs. transverse stress on a single wire

The WASP concept

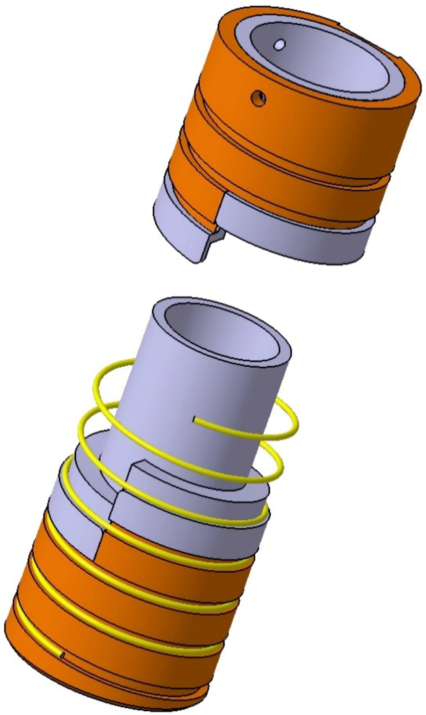

B. Seeber et al., IEEE TASC 17 (2007) 2643

G. Mondonico et al., SuST 25 (2012) 115002

4-WALL + impregnation

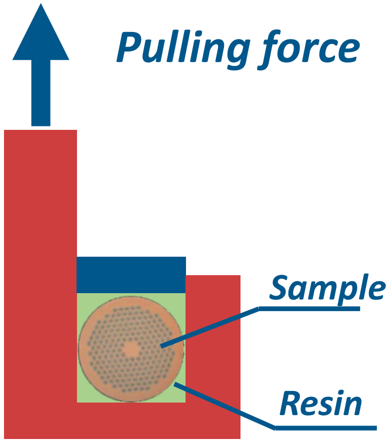

UNIVERSITÉ DE GENÈVE FACULTÉ DES SCIENCES CERN collaboration agreement K1629/TE (2009-2012)

I_c vs. transverse stress

Powder-In-Tube Nb_3Sn wire + epoxy L

# of subelements	Cu/non-Cu	Diameter	I_c(16 T)
192	1.22	1.0 mm	340 A

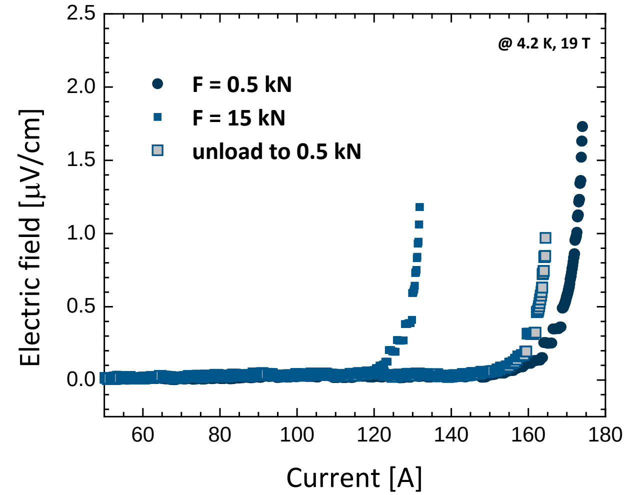

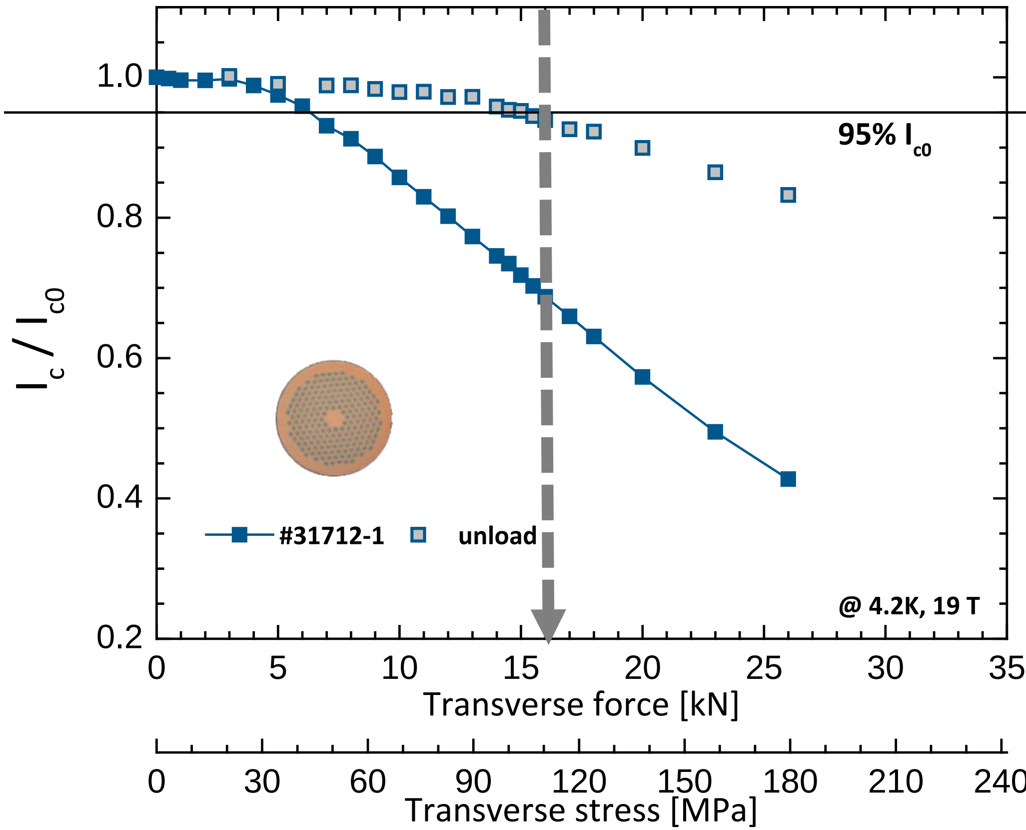

The irreversible limit is defined at the force level leading to a 95% recovery of the initial I_c after unload

Here

$$F_{irr}(B=19T) = 16\ kN$$

The corresponding irreversible stress limit is

$$\sigma_{irr}(B=19T) = 110\ MPa$$

where

$$Stress = \frac{Force}{groove\ length \times groove\ width}$$

Irreversible degradation phenomena

Two mechanisms govern the irreversible degradation of the critical current

- ***Formation of cracks in the Nb_3Sn filaments due, for instance, to the stress concentration at the voids formed during the reaction heat treatment***

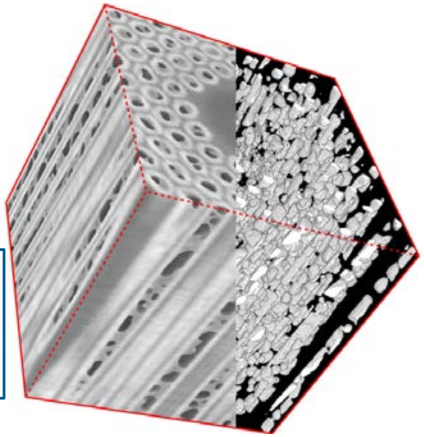

Cracks generate a reduction of the current carrying cross section ⇒ I_c^{unload}/I_{c0} is independent of the magnetic field

- ***Plastic deformation of the matrix and residual stress on the Nb_3Sn filaments.***

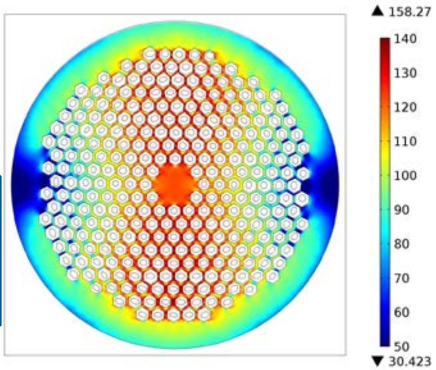

Residual stress induces a permanent reduction of B_{c2} after unload ⇒ I_c^{unload}/I_{c0} depends on of the magnetic field

Field dependence of the irreversible stress limit

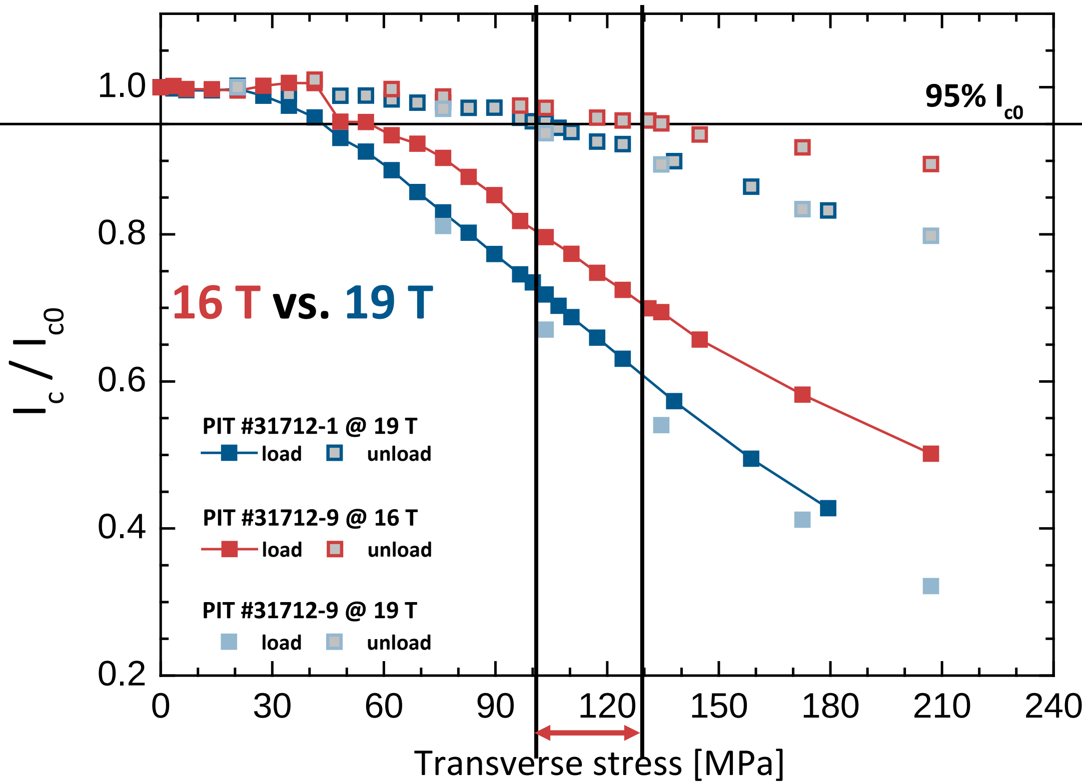

$\Delta\sigma_{irr}$ (19 T → 16 T) ≈ +20 MPa

I_c^{unload}/I_{c0} depends clearly on of the magnetic field !!

σ_{irr} at 16 T increases by ~20 MPa compared to 19 T

Residual stress on Nb_3Sn due to the plastic deformation of the matrix dominates the irreversible degradation

Field dependence of the irreversible stress limit

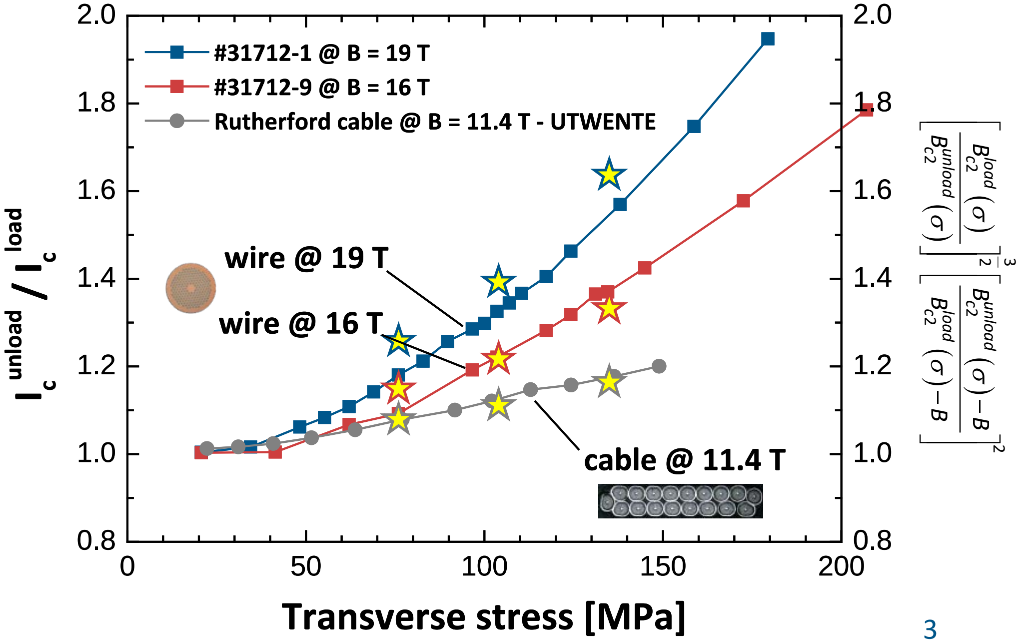

A simple model, based only on the effects of residual stress, reproduces the experimental dependences on field and stress

It proves also that the experiments performed on the single wire are consistent with those on cables

$$\frac{I_c^{unload}}{I_c^{load}}(B,\sigma)=\left[\frac{B_{c2}^{load}(\sigma)}{B_{c2}^{unload}(\sigma)}\right]^{\frac{3}{2}}\left[\frac{B_{c2}^{unload}(\sigma)-B}{B_{c2}^{load}(\sigma)-B}\right]^{2}$$

L. Gamperle et al., arXiv: 1909.13543

To conclude…

65 years after the discovery there is a revamp of interest for Nb_3Sn

In particular, the FCC study is driving Nb_3Sn towards its ultimate performance

- *material with refined grains and high B_{c2} is produced in several laboratories around the world*
- *practical solutions to implement this technologyin industrial wires are being developed*

But there is still work to do also on other properties of the conductors, e.g. the tolerance to stress

- *Developing tailored heat treatments to control size and distribution of the voids in the filaments*
- *Optimizing the filament layout in the wire by using FEM, to predict the redistribution of mechanical loads between superconductor and matrix*

Not at the exclusive benefit of high energy physics, but also for fusion (DEMO), NMR and medical accelerators


Thank you for the attention !
Carmine SENATORE
carmine.senatore@unige.ch
http://supra.unige.ch
UNIVERSITÉ DE GENÈVE
FACULTÉ DES SCIENCES
DQMP
http://supra.unige.ch